Microchimica Acta (2019) 186: 583
https://doi.org/10.1007/s00604-019-3688-y

REVIEW ARTICLE

The fluorescence mechanism of carbon dots, and methods for tuning their emission color: a review

Fanyong Yan[1] · Zhonghui Sun[1] · Hao Zhang[1] · Xiaodong Sun[1] · Yingxia Jiang[1] · Zhangjun Bai[1,2]

Received: 9 April 2019 / Accepted: 7 July 2019 / Published online: 29 July 2019

Abstract

Carbon dots (CDs) display tunable photoluminescence and excitation-wavelength dependent emission. The color of fluorescence is affected by electronic bandgap transitions of conjugated π-domains, surface defect states, local fluorophores and element doping. In this review (with 145 refs.), the studies performed in the past 5 years on the relationship between the fluorescence mechanism and modes for modulating the emission color of CDs are summarized. The applications of such CDs in sensors and assays are then outlined. A concluding section then gives an outlook and describes current challenges in the design of CDs with different emission colors.

Keywords Carbon dots · Conjugated π-domains · Surface defect · Fluorophores · Elements doping · Surface groups · Quantum yield · Decay times · Precursors · Solvents

Introduction

Carbon dots (CDs) have a typical size of less than 10 nm [1, 2]. CDs consist of two parts: one is a spherical-like core formed by stacking multiple graphene fragments in an ordered or disordered manner; the other is rich functional groups distributed on the surface of CDs [2, 3]. Notably, CDs exhibit tunable photoluminescence (PL), multi-color emission associated with excitation [4–6], low toxicity and good biocompatibility [7–11]. All these unique properties make CDs have potential applications in biomedicine, sensing and optoelectronics [12–16].

The modulating the color-emitting of CDs have always been the focus of attention [17, 18]. Once the chemical structure of CDs is well controlled during the preparation process, it is possible to clarify the factors affecting the fluorescence mechanism of CDs and ultimately regulate the color-emitting of CDs. In general, the fluorescence behavior of CDs is affected by the relationship between the carbon core and surrounding chemical groups [19]. For some CDs with large conjugated π-domains and few surface chemical groups, the band gap of conjugated π-domains is considered to be the carbon-core states fluorescence center. By adjusting the size of the conjugated π-domains, the color-emitting of CDs can be adjusted. For surface defect states mechanism, the surface chemical groups of CDs have various energy levels and result in more emissive traps. A higher degree of surface oxidation can lead to more surface defects and the red-shift of emission wavelengths. For the molecule states mechanism, the fluorescence center is composed of organic fluorophores formed by small-molecule carbonization. Some fluorescent small molecules or fluorophores are attached to the surface or interior of carbon skeleton and show emission directly. Moreover, doping is an effective method for modulating the color-emitting, QY and decay lifetime of CDs. There are many reviews papers on CDs

✉ Fanyong Yan
yfany@163.com

[1] State Key Laboratory of Separation Membranes and Membrane Processes/National Center for International Joint Research on Separation Membranes, School of Chemistry and Chemical Engineering, Tianjin Polytechnic University, Tianjin 300387, People's Republic of China

[2] State Key Laboratory of Chemo/Biosensing and Chemometrics, Provincial Hunan Key Laboratory for Cost-effective Utilization of Fossil Fuel Aimed at Reducing Carbon dioxide Emissions, College of Chemistry and Chemical Engineering, Hunan University, Changsha 410082, Hunan, China

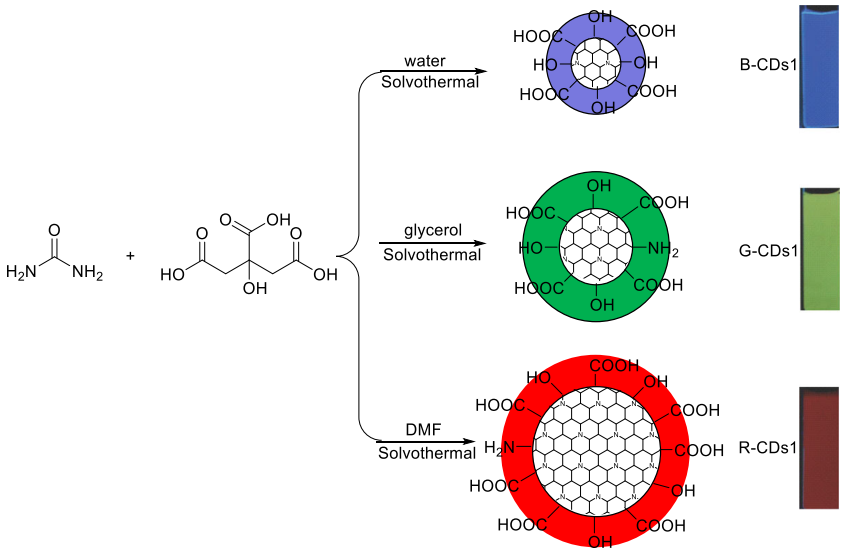

Fig. 1 Schematic presentation of CDs1 fabrication

but the relationship between the fluorescence mechanisms and color-emitting modulation of CDs has not been systematically summarized so far [2, 20–23].

The present review highlighted the fluorescence mechanism and the color-emitting modulation methods of CDs, as well as resulting fluorescence behaviors and applications. We mainly discussed the modulation of CDs with blue-, green-, yellow-, red-light emission and multicolor and mentioned their applications. This paper will provide a theoretical basis for the structure and properties control of CDs.

Fluorescence mechanism of CDs

Bandgap transitions of conjugated π-domains

A major feature of CDs is the quantum confinement effect (QCE), which appears when CDs are smaller than the exciton Bohr radius. The QCE refers to the valence band and conduction band change from the continuous energy band to discrete energy level and the band gap increases with the decrease of the three-dimensional size of the material at the nanometer level, which results in the band gap transition in the ultraviolet-visible region and greatly improves the fluorescent quantum yield (QY).

For some CDs with large conjugated π-domains and few surface functional groups, fluorescence is essentially derived from the QCE of conjugated π electrons, and the band gap of conjugated π-domains is considered to be the carbon-core states fluorescence center [24–26]. The larger the size of CDs conjugated π-domain, the smaller the band gap and the more redshift of the emission peak. The conjugated π-domains with confined size results in the separation of the valence band of the CDs from the conduction band, and the conduction band electrons directly transition to an empty state of the valence band, thereby enabling "direct recombination" of electrons and holes, resulting in a so-called band gap fluorescence. The sp^2 carbon clusters in CDs are dispersed in the sp^3 carbon skeleton, so the optical properties of CDs are determined by the π-electron state of the sp^2 carbon cluster [27–29]. Since the electron energy levels of π and π* in the sp^2 carbon cluster are affected by the σ and σ* states in the sp^3 carbon skeleton, the radiation transition of the electron-hole pairs in the sp^2 carbon cluster can produce fluorescence. By adjusting the size of the conjugated π-domains, the band gap

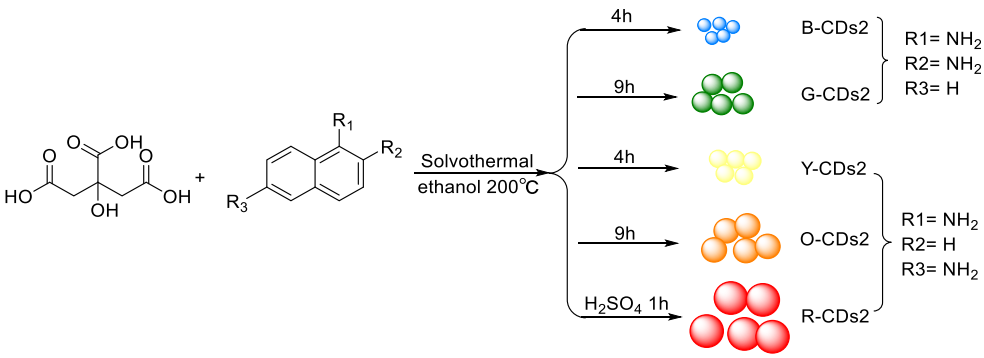

Fig. 2 Schematic presentation of CDs2 fabrication

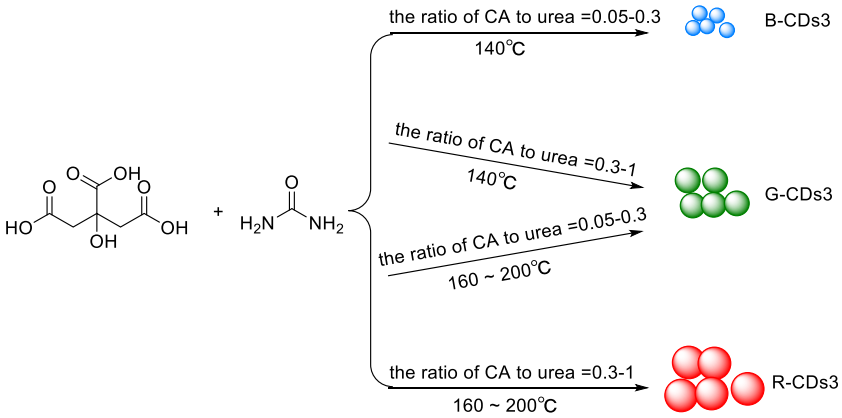

Fig. 3 Schematic representation of CDs3 fabrication

of CDs can be tuned, and it is expected to modulate the color-emitting of CDs.

The size of the conjugated π-domains can be adjusted using different reaction solvents and the color-emitting of CDs can be further modulated. Tian et al. [30] prepared multicolor-emitting CDs1 using citric acid (CA), urea and three different solvents (water, glycerol, and dimethyl formamide) via a solvothermal method. The solvents control the dehydration and carbonization processes of precursors, resulting in the formation of conjugated π-domains of different sizes in CDs1, which in turn leads to different emission colors from blue to red. They further prepared CDs1 phosphors/ PDMS composites and WLEDs by covering red and green CDs1 phosphors on luminescent blue InGaN chips (Fig. 1).

The color-emitting of CDs can be tuned by varying precursors and reaction time. Yuan et al. [31] synthesized multicolor-emitting CDs2 by controlling the fusion and carbonization of CA and diaminonaphthalene (DAN). The emission peaks of the blue, green, yellow, orange, and red CDs were centered at 430, 513, 535, 565 and 604 nm, respectively. The QYs were 75%, 73%, 58%, 53% and 12%, respectively. CDs2 showed average sizes of about 1.95, 2.41, 3.78, 4.90 and 6.68 nm,

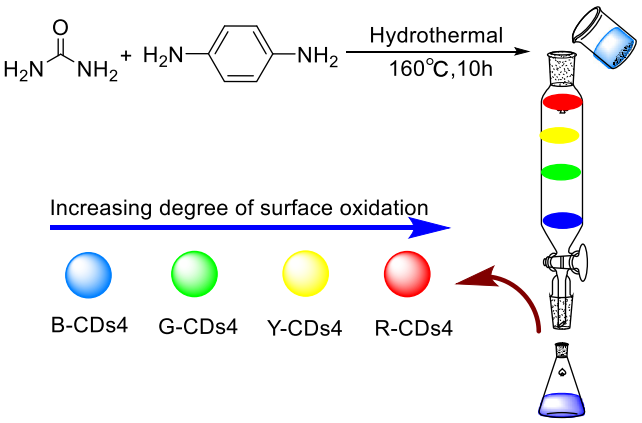

Fig. 4 Schematic presentation of CDs4 fabrication and its fluorescence mechanism

respectively. As the size of CDs2 increases(conjugated π-domain increases), the bandgap decreases gradually, resulting in the tunable fluorescence emission from blue to red. The monochrome LEDs from blue to red and WLEDs were respectively prepared using CDs2 and CDs2 blended PVK as the emission layer (Fig. 2).

The color-emitting of CDs also can be modulated by changing the molar ratio of precursors and the reaction temperature. More recently, Miao et al. [23] prepared the multicolor-emitting CDs3 by using different molar ratios of CA to urea at different temperatures. The emission of CDs3 can be adjusted from 430 to 630 nm by controlling the degree of graphitization and the number of surface -COOH groups. The QYs of the three CDs3 of blue, green and red were 52.6%, 35.1% and 12.9%, respectively.

With the increase of the effective conjugation length and the surface -COOH groups, the band gap caused by π-electron delocalization in the sp^2 domain is reduced, and the emission wavelength is red-shifted. CDs3 can be evenly dispersed into epoxy resins to form transparent CDs/epoxy composites for multicolor WLED (Fig. 3).

The bandgap transitions of conjugated π-domains to describe the fluorescence of CDs is actually based on the premise of single-layer graphene fragments, which is not enough to explain the complex structure of multiple graphene fragments stacked like CDs. Therefore, the explanation of the fluorescence properties of CDs based on nanometer size and quantum size effects has certain limitations. Quantum size effects is often used in conjunction with surface defect states.

Surface defect states

Another fluorescence mechanism is that the fluorescence of CDs is dominated by its rich surface defect states. The surface defect refers to a boundary region or a spherical shell that is distinct from the carbon core region or body. The spheroidal region contains various chemical groups derived from sp^2 and sp^3 hybrid carbons, or other surface functional groups [32, 33], or dangling bonds. Due to the diversity and

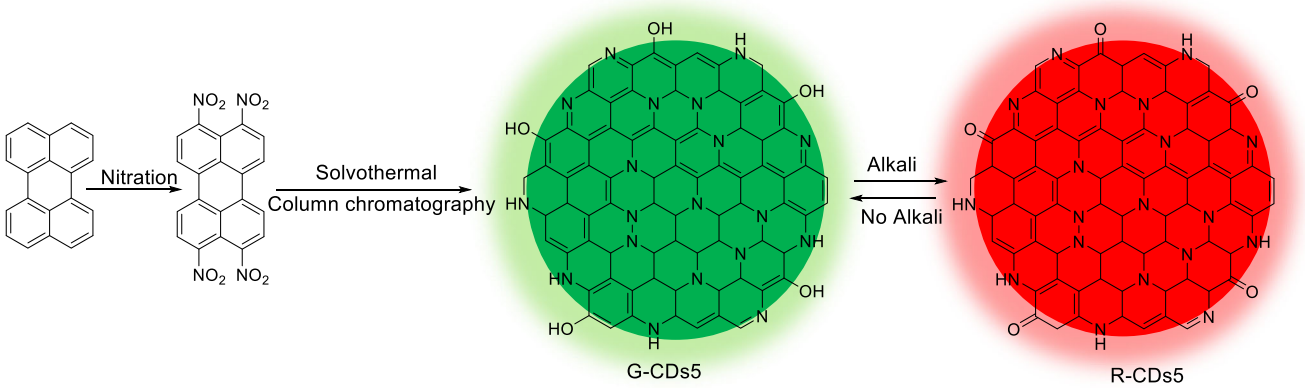

Fig. 5 Schematic presentation of CDs5 fabrication

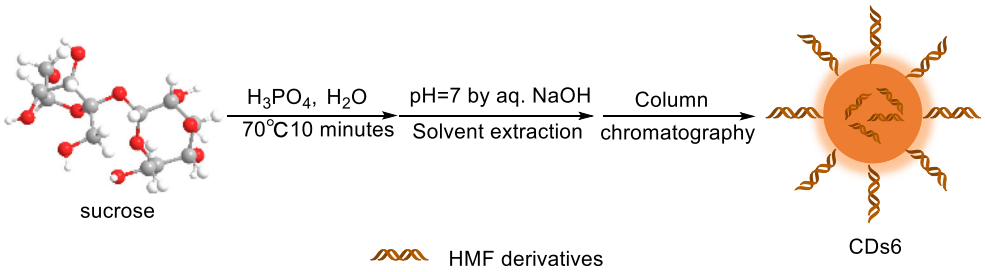

Fig. 6 Schematic presentation of CDs6 fabrication

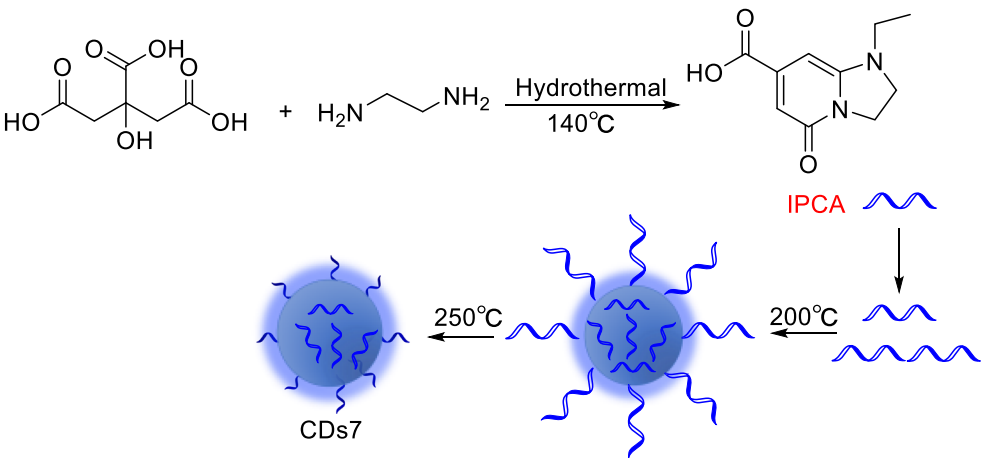

Fig. 7 Schematic presentation of CDs7 fabrication

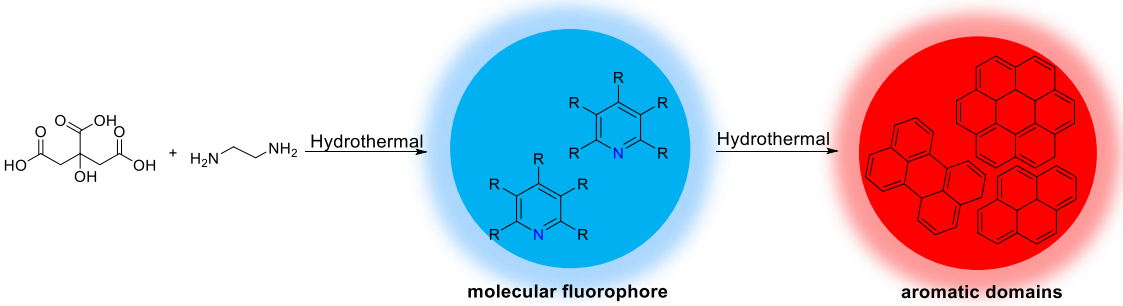

Fig. 8 Schematic presentation of CDs8 fabrication

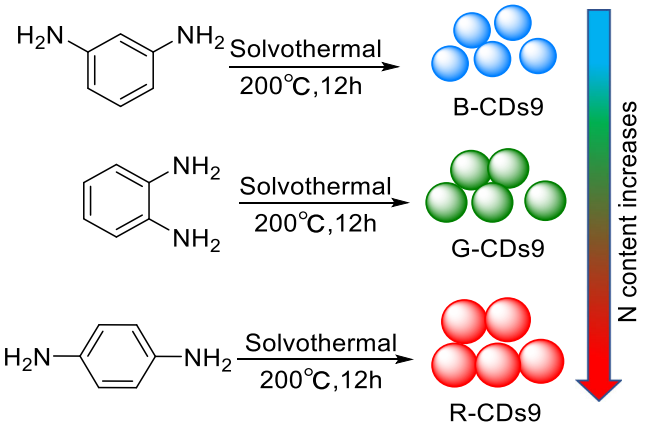

Fig. 9 Schematic presentation of CDs9 fabrication and its fluorescence mechanism

complexity of surface defect states, fluorescence originating from surface defect states is characterized by pleochroism and excitation-dependent luminescence. Surface defects are mainly generated by surface oxidation and can act as a capture center for excitons, resulting in surface defect state fluorescence [34, 35].

Surface defect fluorescence is caused by radiation relaxation from the excited state to the ground state. sp^3 and sp^2 hybrid carbon on the surface of CDs and other surface defects can lead to multicolor emissions of their local electronic states. When the light of a specific wavelength illuminates CDs, the photons whose energy satisfies the optical band gap will transition and accumulate in the adjacent surface defect traps, and return to the ground state to emit visible light of different wavelengths. The higher the degree of surface oxidation of CDs, the more surface defects and emission sites, resulting in the red-shift of emission wavelength [36–38].

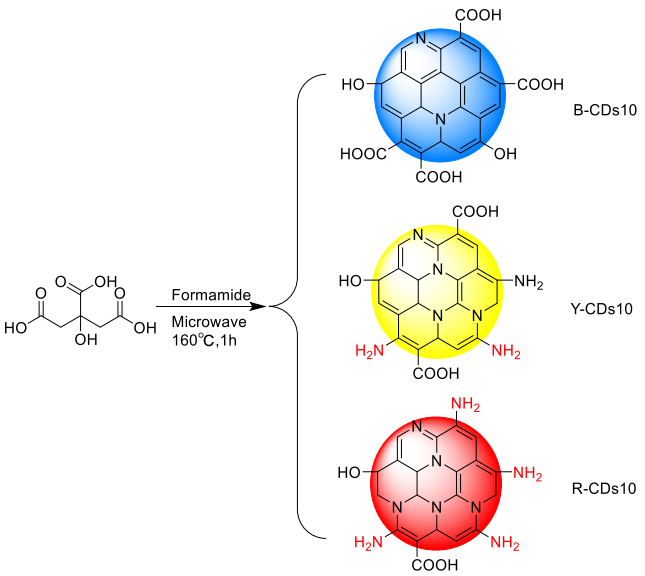

Fig. 10 Schematic presentation of CDs10 fabrication

The surface state is not composed of isolated chemical groups, but a fluorescence center formed by the synergy of carbon core with associated chemical groups. Among them, some groups are fluorescence activation state or silence state under a certain condition. Functional groups have different energy levels and may produce a series of emission traps [39–41]. The energy levels of functional groups may be related to their ability to supply electrons. The stronger the ability of functional groups to provide electrons, the higher the energy they generate. Obviously, the emission wavelength can be adjusted by changing the chemical groups on the surface of CDs.

Different degrees of surface oxidation will facilitate the color-emitting modulation of CDs. Ding et al. [42] synthesized multicolor-emitting CDs4 using p-phenylenediamine and urea through a hydrothermal method. After column chromatography, CDs4 exhibit excitation-independent fluorescence from blue to red. The QYs of R-CDs4 was 24%. Different degrees of oxidation of the CDs4 resulted in different surface states, and the band gap gradually decreased, which ultimately determined the fluorescence red shift. Because of their excellent fluorescence properties and low cytotoxicity, CDs4 can be used to image HeLa cells and live nude mice (Fig. 4).

By changing the functional groups on the surface can tune the color-emitting of CDs. Yuan et al. [43] synthesized green light-emitting G-CDs5 and red light-emitting R-CDs5 using perylene as the precursor. The QYs of G-CDs5 and R-CDs5 were 81% and 80%, respectively. The alkali can cause the increase in the quinone structure of R-CDs5, resulting in an electron-rich property. Rich electrons can raise HOMO to higher energy levels, causing a red shift of fluorescence. This highly efficient G-CDs5/MTES and R-CDs5/APTES can be made by doping G-CDs5 and R-CDs5 into MTES and APTES with QYs of 80% and 78%, respectively. Integrating G-CDs5/MTES and R-CDs5/APTES on a blue LED chip, a blue pumped CDs phosphor based three-color warm WLED was prepared (Fig. 5).

Surface states mechanism was considered to be the key fluorescence mechanism of CDs, which provide a primary way to modulate the color-emitting of CDs through controlling the surface states. However, we cannot ignore the role of the carbon-core states in fluorescence emission, especially in short wavelength regions.

Effects of fluorescent molecules or fluorophores

The fluorescent molecules or fluorophores in CDs are small organic molecules or chromophores similar to dye molecules. These fluorescent small molecules or fluorophores are connected on the surface or interior of the carbon backbone and can exhibit fluorescence emission directly [44]. Such molecular fluorescence mechanisms are more common in the

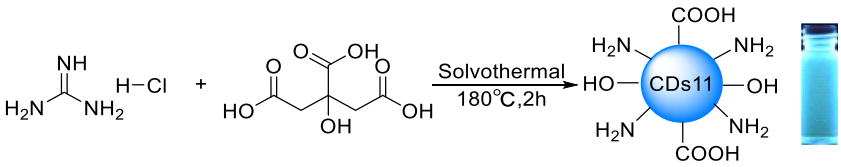

Fig. 11 Schematic presentation of CDs11 fabrication

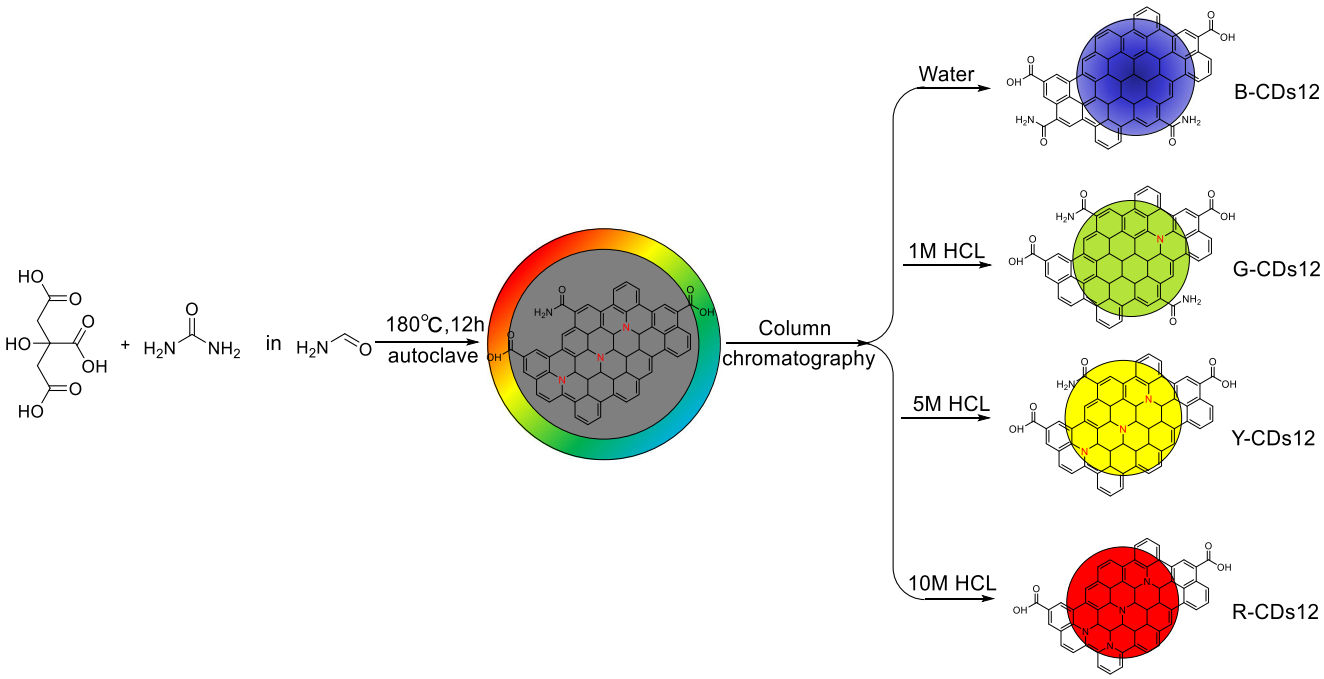

Fig. 12 Schematic presentation of CDs12 fabrication

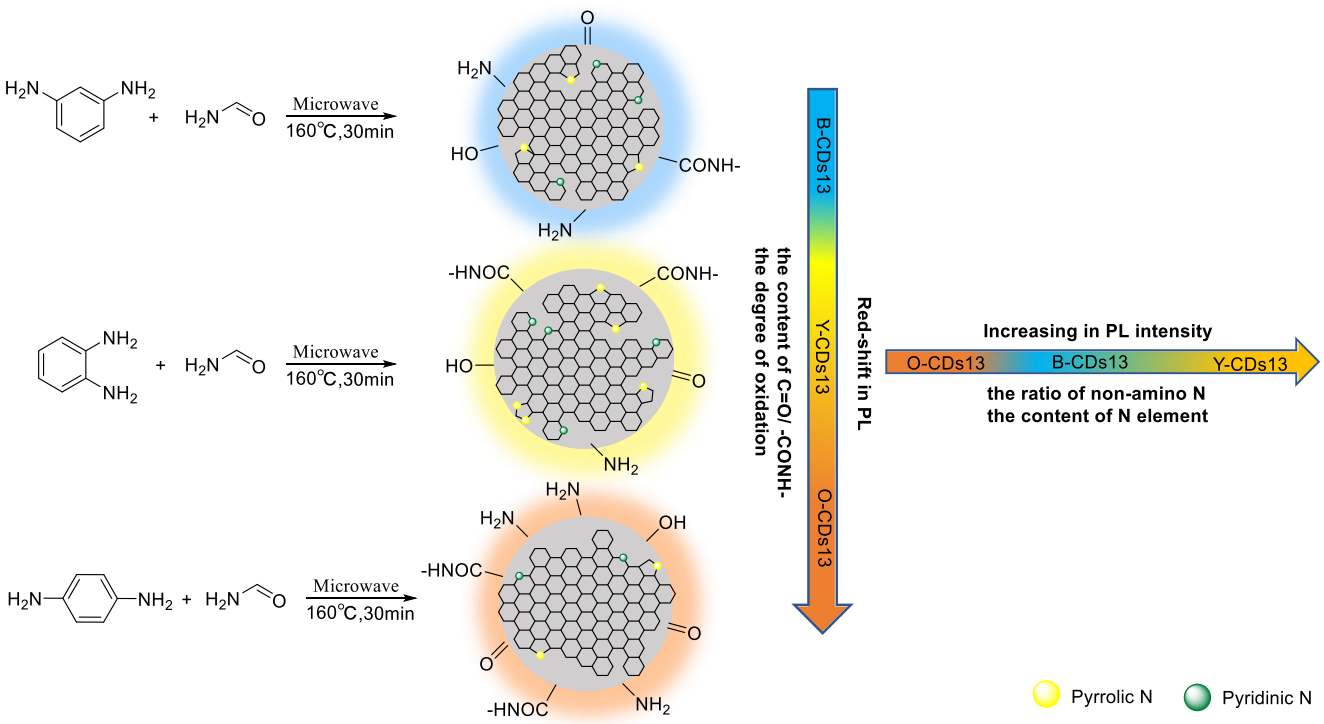

Fig. 13 Schematic presentation of CDs13 fabrication and its fluorescence mechanism

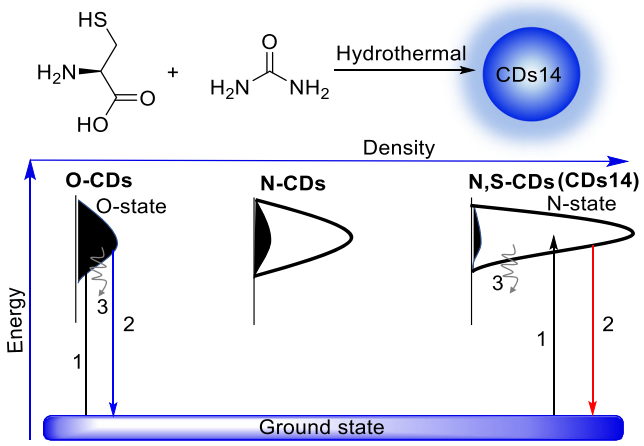

Fig. 14 Schematic presentation of CDs14 fabrication and its fluorescence mechanism

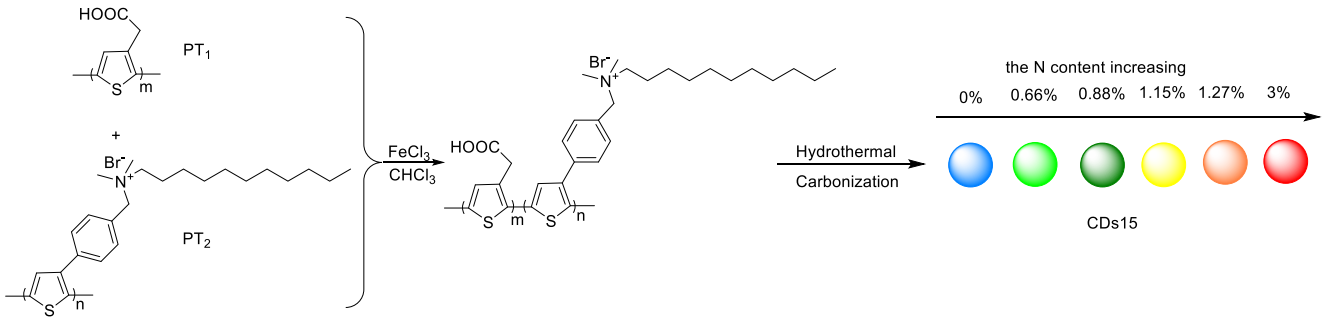

Fig. 15 Schematic presentation of CDs15 fabrication and its fluorescence mechanism

Fig. 16 Schematic presentation of CDs16 fabrication

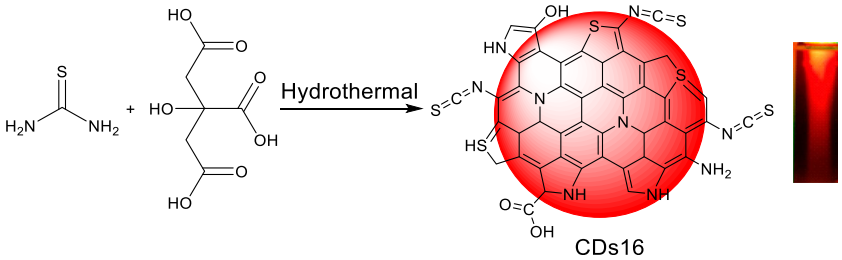

Fig. 17 Schematic presentation of CDs17 fabrication

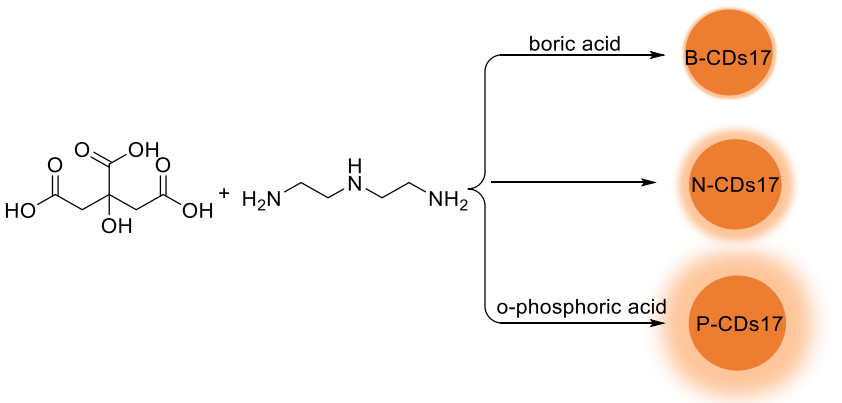

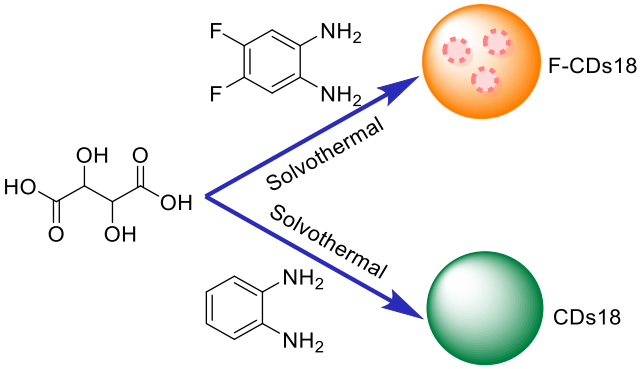

Fig. 18 Schematic presentation of CDs18 and F-CDs18 fabrication

Fig. 19 Schematic presentation of Se-CDs19 fabrication

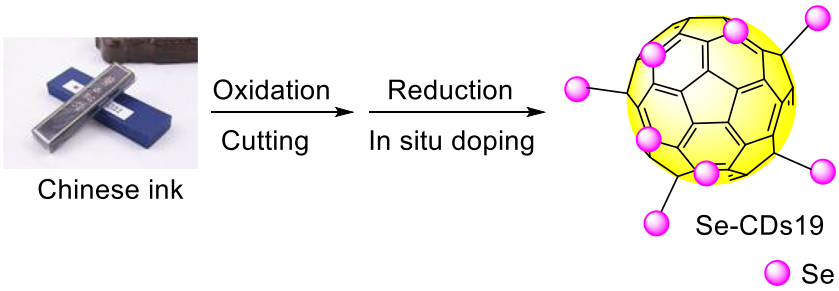

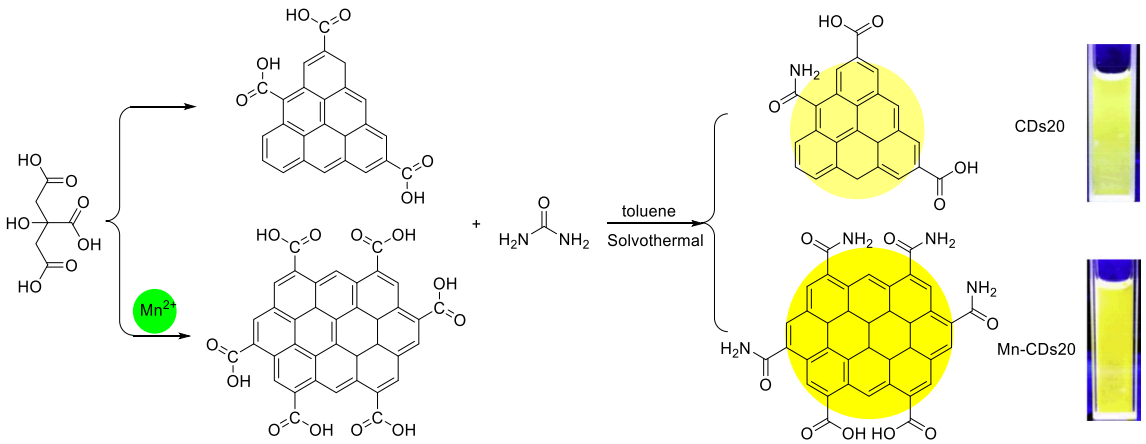

Fig. 20 Schematic presentation of CDs20 and Mn-CDs20 fabrication

Fig. 21 Schematic presentation of Cu-CDs21 fabrication

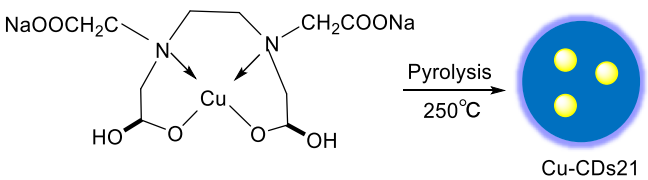

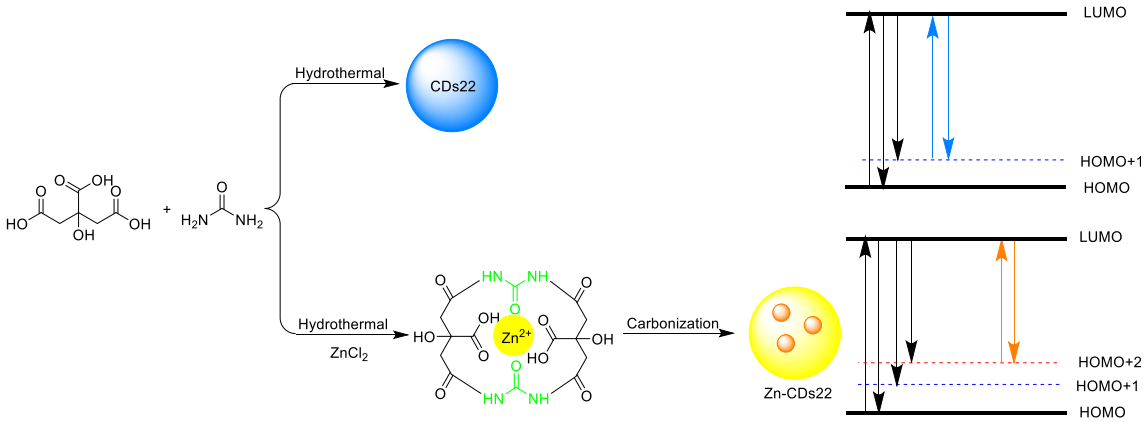

Fig. 22 Schematic presentation of CDs22 and Zn-CDs22 fabrication and its fluorescence mechanism

preparation of CDs by small molecule condensation/carbonization [45]. As the carbonization temperature or time increases, the carbon core is formed by dehydration of the initial molecule or formation of a fluorophore. In general, the QYs of fluorescent molecules in such CDs is much higher than the band gap fluorescence efficiency caused by QCE of the conjugated π-domains, but the molecular luminescence stability is lower than that of band gap fluorescence.

Based on the molecule states fluorescence mechanism, Gude et al. [46] prepared orange-red light-emitting CDs6 from easily available sources like sucrose, fructose and glucose at low temperature of 70 °C. CDs6 are composed of aggregated hydroxymethylfurfural (HMF) derivatives and exhibit excitation wavelength independent fluorescence emission at 590 nm. There is only one type of chromophore (HMF derivatives) in CDs6. Aggregated HMF derivatives are responsible for fluorescence and a large Stokes shift (~ 150 nm) of CDs6 (Fig. 6).

The interaction between bandgap fluorescence and molecular fluorescence further improves the fluorescence mechanism and has a large effect on the color-emitting of CDs [47]. Song et al. [48] fabricated CDs7 using CA and ethylenediamine (EDA) as precursors. A bright blue fluorophore (imidazo[1,2-a]pyridine-7-carboxylic acid, 1,2,3,5 -tetrahydro-5-oxo-, IPCA) was obtained by separation of CDs7. A separate fluorophore IPCA attached to the surface

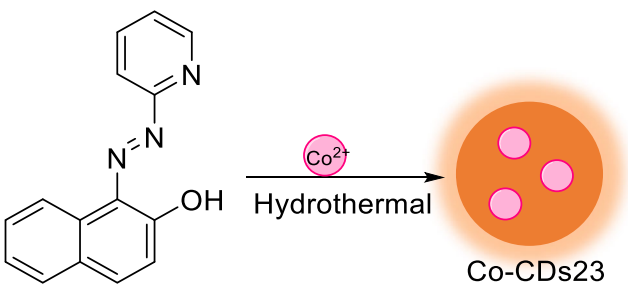

Fig. 23 Schematic presentation of Co-CDs23 fabrication

or inside of carbon core is the true molecular state fluorescence center. In CDs with lower carbonization temperatures, molecular fluorescence dominates, while in CDs with higher reaction temperatures, carbon core plays a dominant role. As the temperature increases, a part of the molecular fluorophore is consumed to form a crystalline carbon core. IPCA has polar groups, rigid ring structure and low cytotoxicity, and has broad application prospects in biomedicine (Fig. 7).

Afterwards, Ehrat et al. [49] synthesized CDs8 by pyrolysis of CA and EDA at different synthesis times. In the initial phase, the molecular fluorophore dominates the blue fluorescence of CDs8. However, over time, the aromatic domains form and increase, causing the fluorescence red shift. A molecular fluorophore may serve as a seed for the formation of aromatic domains (Fig. 8).

Effects of doping with other elements

Pristine CDs containing only C and O elements usually emit blue fluorescence and have low QYs, and most require further surface modification or functionalization to improve luminous efficiency, which often limits the application and development of CDs. Other element doping can introduce new surface properties to CDs and alter structural defects, surface function groups, and interactions among carbon atoms with their neighboring atoms [50, 51]. These new surface states can suppress or eliminate the original O-states and facilitate a high yield of radiative recombination, resulting in doped CDs with higher QYs and excitation-independent emissions. The doped elements might also be embedded within the carbon core structure of CDs to create new energy levels or change their initial band gap. In summary, doping elements can effectively modulate the color-emitting of CDs and contribute to a deeper understanding of the fluorescence mechanism of CDs.

The QY refers to the fraction of the excited state molecule that returns to the ground state by emitting fluorescence. In other words, the QY is the ratio of emitted photons to absorbed

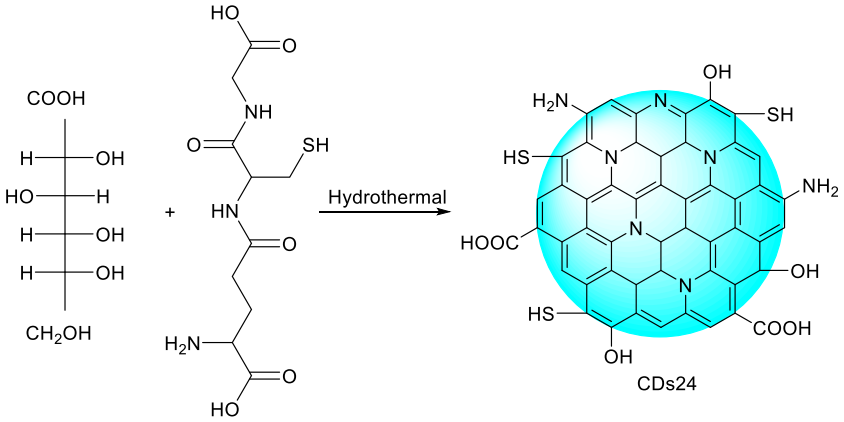

Fig. 24 Schematic presentation of CDs24 fabrication

photons. The QY of CDs is influenced by different synthetic method, precursor, surface passivation, and element doping. Element doping (with nitrogen, sulfur, other heteroatoms and metal ions) can well control the band gap and electron local density of CDs, greatly improving their QY. Different surface states derived from doping effects would have a primary influence on the QY of CDs.

The PL decay lifetime of CDs represents the time that CDs spend in the excited state before photon emission returns to the ground state. It is an intrinsic property of CDs, which is usually on the low nanosecond scale. It also can be tuned by different fabrication methods, precursors, surface passivation, or doping with elements. Element doping appears to be an important factor affecting the PL decay lifetime of CDs. Due to element doping, the surface of CDs develops passivated defects, resulting in a longer PL decay lifetime.

The level of QY and the length of decay lifetime are two important indicators for measuring the potential of CDs in bioimaging and sensing. Therefore, in order to widely apply CDs in the field of biological imaging and sensing, QY needs to be improved, and the decay life also needs to be extended.

Effects of nitrogen doped CDs and nitrogen morphology

Since the radius of the N atom is similar to that of the C atom and the N atom is easily incorporated into the carbon material skeleton, the N-doped CDs are the most studied and most potential doping system [52–54]. The effect of N doping on the fluorescence properties of CDs is mainly divided into two aspects [55–57]: the red-shift of emission wavelength and the fluorescence QY increase [58, 59]. The rearrangement of electron hole and radiation theory is mainly used to explain the fluorescence mechanism of heteroatom-doped CDs. The nitrogen atom produces a new surface state energy level resulting in a red-shift of emission wavelength. Nitrogen-doped surface states can facilitate a high yield of radiative recombination and depress non-radiative recombination. The

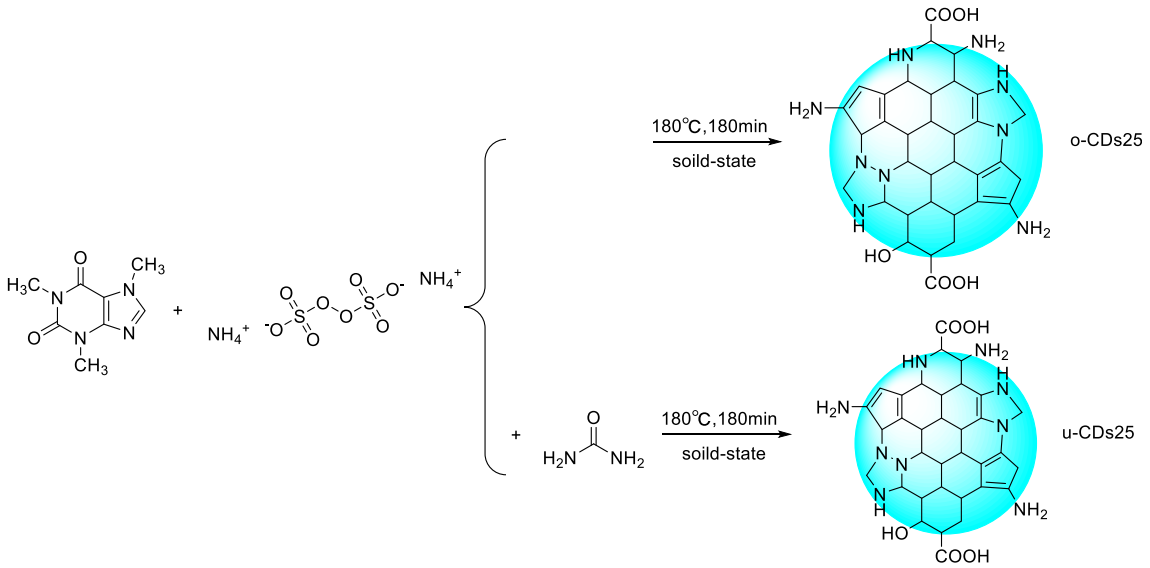

Fig. 25 Schematic presentation of CDs25 fabrication

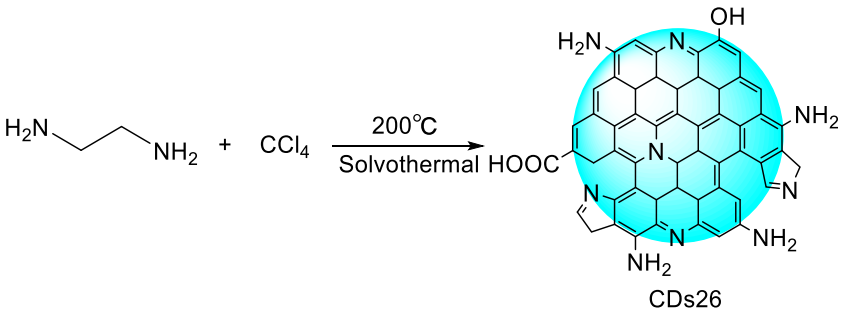

Fig. 26 Schematic presentation of CDs26 fabrication

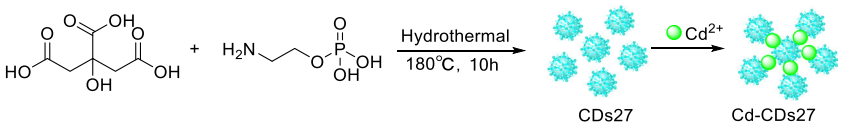

Fig. 27 Schematic presentation of CDs27 fabrication

Table 1 An overview on blue-emitting carbon dots

Types	Particle composition	Particle Size(nm)	Ex/Em (nm)	QY (%)	Decay times(ns)	Ref
CDs24	C, H, O, N, S	2.6 ± 4	330/471	7.2	–	[91]
o-CDs25	C, H, O, N, S	6	340/400	38	–	[91]
u-CDs25	C, H, O, N, S	13	360/426	69	–	
CDs26	C, H, O, N	7	317/390	36.3	–	[93]
CDs27	C, H, O, N, P	1.6	325/435	8.17	–	[94]
Cd-CDs27	C, H, O, N, P, Cd	3	–	–	–	

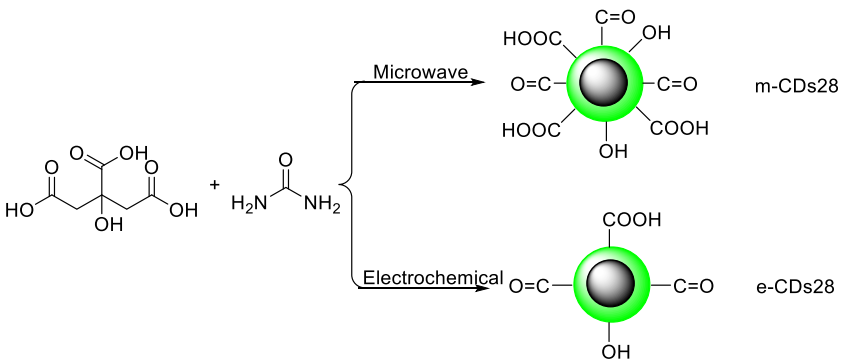

Fig. 28 Schematic presentation of m-CDs28 and e-CDs28 fabrication

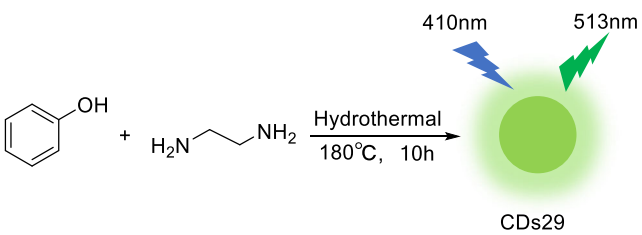

Fig. 29 Schematic presentation of CDs29 fabrication

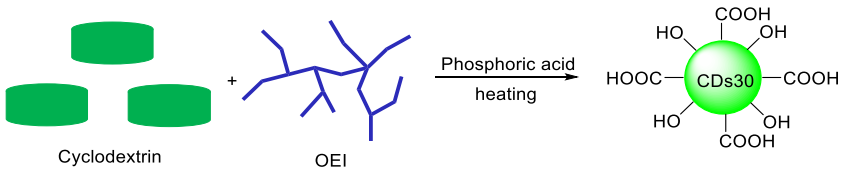

Fig. 30 Schematic presentation of CDs30 fabrication

electron-donating amino-groups on the CDs surface can enhance the conjugation degree of conjugated systems, increasing the electron transition from the ground state to the lowest excited singlet state, and thus contribute to higher QY indirectly of the CDs [60–62].

Differences in nitrogen content caused by doping can modulate the color-emitting, QY and decay lifetime of CDs. Jiang et al. [63] synthesized CDs9 using three different phenylenediamine isomers in ethanol through a solvothermal method. Under 365 nm UV excitation, CDs9 emitted red, green and blue fluorescence in solution and in the polymer matrix. The difference in the color-emitting, QY and decay lifetime of CDs9 was due to the increase in nitrogen content (B-CDs9, G-CDs9, and R-CDs9 were 3.69%, 7.32%, and 15.57%, respectively). The maximum emission wavelength of B-CDs9, G-CDs9 and R-CDs9 were 435, 535, and 604 nm under excitation at 365 nm, respectively. The fluorescence QY was 4.8, 17.6 and 26.1%, respectively. The decay lifetime was 0.99, 4.44 and 9.39 ns, respectively. CDs9 can prepare multicolor emission PVA films, multicolor displays and multiplexed biological imaging reagents (Fig. 9).

N-related functional groups produced by doping will have a great effect on the color-emitting of CDs. Pan et al. [64] prepared full-color emission CDs10 via microwave assisted heating CA and formamide solution at 160 °C for 1 h. CDs10 exhibited excitation-independent fluorescence from blue to red. The QY of CDs10 was 11.9%, 16.7% and 26.2% when the excitation was 360, 450, and 540 nm, respectively. The blue light-emitting of CDs10 should come from an aromatic structure, while the green and red light-emitting are due to the presence of C=N/C=O and C-N related functional groups. CDs10 can be used to detect a variety of metal ions, and as biomarker reagents for deep tissue imaging (Fig. 10).

The color-emitting of CDs can be modulated by controlling nitrogen-doped surface states. The QY increased and fluorescence lifetime was prolonged as the nitrogen content increases. Yuan et al. [65] prepared CDs11 with the nitrogen-content changes from 5.5% to 19.9% by controlling the molar ratios of CA and guanidine hydrochloride. CDs11–1, CDs11–2 and CDs11–3 showed emission-dependent emission, while CDs11–4, CDs11–5 and CDs11–6 with high surface -NH_2 groups density showed excitation-independent emission. The surface states of CDs11–6 be completely passivated by electron-donating -NH_2 groups, leading to single energy level and showing high fluorescence emission efficiency. Nitrogen-doped surface states promoted a high yield of radiative recombination of the surface-trapped electrons and holes in CDs11. Furthermore, tunable fluorescent CD11 has been used as an effective fluorescent probe for semi-quantitative monitoring of intracellular Hg^{2+} (Fig. 11).

The complex N-doping process leads to the existence of multiple nitrogen species in the structure of CDs, and the different configurations of N atoms have unlike effects on the different properties of N-doped CDs [66]. The nitrogen forms present in CDs can be mainly classified into four types: amino type, pyrrole type, pyridine type and graphite type. The amino N is distributed on the surface of CDs, while the pyrrole N and pyridine N can be distributed at the edge and center of graphene structure, and the graphite N is regularly doped in the graphene skeleton. The fluorescence properties of CDs can be further demonstrated by the clear nitrogen form and the distribution. Most researchers believe that amino groups can improve the fluorescence of CDs by self-passivation [67, 68].

The increasing graphite nitrogen is beneficial for modulating the color-emitting of CDs. The aromatic amine or terminal aliphatic amine of CA can cause C-N cross-linking during carbonization to form graphite nitrogen structure, which is beneficial for red light-emitting of CDs. To further investigate the relationship between nitrogen form and the fluorescence properties of CDs, Hola et al. [69] prepared multicolor emission CDs12 using urea and CA in formamide via a solvothermal process. CDs12 were separated by column chromatography based on differences in surface charge. In water, the QYs of B-CDs12, G-CDs12, Y-CDs12, and R-CDs12

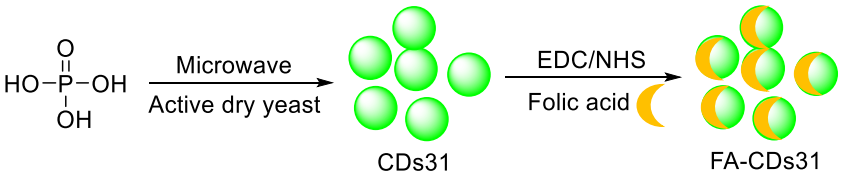

Fig. 31 Schematic presentation of CDs31 and FA-CDs31 fabrication

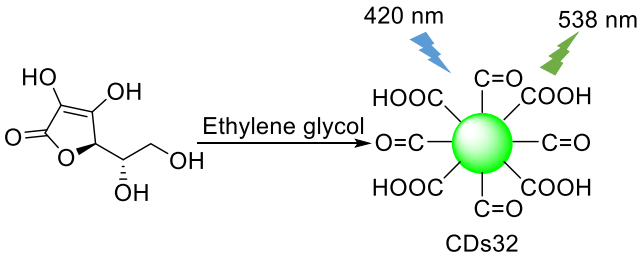

Fig. 32 Schematic presentation of CDs32 fabrication

were 13.3%, 10.0%, 11.6%, and 4.0%, respectively. The increasing graphite nitrogen in CDs12 caused the energy gap decrease, finally resulting in the red-shift of emission wavelength. R-CDs12 had great application potential in the field of biomedicine (Fig. 12).

The number and speciation of N-functional groups on the surface are related to modulating the color-emitting of CDs. Liu et al. [70] synthesized blue, yellow and orange fluorescence CDs13 using m-phenylenediamine, o-phenylenediamine and p-phenylenediamine as precursors by microwave method. CDs13 showed wavelength-independent excitation. The QYs of three CDs13 were 14.3, 45 and 7.5%, respectively. The non-amino N can break the conjugated structure, creating many defect states to produce more polyaromatic structures, and finally enhance fluorescence. The C=O/ -CONH- groups can give rise to local isolation that will induce deformations in the plane of CDs13, thus cause the energy gap decrease, finally resulting in the red-shift in emission. Moreover, CDs13 have been applied in multicolor cellular imaging, starch/CDs composite phosphors and LEDs illumination (Fig. 13).

Effects of nitrogen and sulfur co-doped CDs

In addition to the N element, other types of non-metallic element doped CDs have also been reported, but the scale of study is far less than that of N-doped CDs. S-doped CDs are the second type of doped CDs that occur after N-doping, where the S element may be in the form of a thiol, thioether or sulfonic acid group [71, 72]. The S element that usually alone exists has no significant effect on the fluorescence emission wavelength, which may be related to its difficulty in embedding the carbon skeleton. Since heteroatom co-doping can produce a unique electronic structure, there is a synergistic effect between the N and S doped in CDs. The atomic radius of N and S is closer to C, and the availability of five valence electrons in N and six in S helps to bind N and S with C. The N and S element can increase the probability of electronic transition from the ground state to the excited state, thereby leading to a change in bandgap energy and significantly increasing QY of CDs.

The role of the S atom may be to suppress the surface state of the O atom and stabilize and enhance the surface state of the N atom. Bao et al. [73] synthesized N, S co-doped CDs (CDs14) using l-cysteine and CA as precursors. The maximum emission wavelength of CDs14 is 415 nm under excitation of 345 nm UV light. The fluorescence QY is calculated to be 16.9%. The fluorescence emission of CDs14 is mainly the recombination of electrons and holes caused by surface-doped nitrogen and/or sulfur atoms. The S atom provides a synergistic effect on the function of the N atom, which greatly accelerates the radiation transition of the N-related surface states, resulting in fluorescence dominated by nitrogen-containing functional groups. CDs14 showed good fluorescence activity and low toxicity, and were widely used in bioimaging and other fields (Fig. 14).

Different surface states derived from doping effects would have a vital influence on the modulating the color-emitting of CDs. Guo et al. [74] fabricated multicolor CDs15 with blue to NIR tunable emission at a single excitation wavelength by varying the ratio of PT1 and PT2 in the polythiophene derivatives via hydrothermal method. CDs15 have an average size of about 3–6 nm, good water solubility and low cytotoxicity. The increasing nitrogen content and the introduction of quaternary ammonium structure are the main reasons for tunable emission colors, while the sulfur element plays a synergistic effect. Multicolor CDs15 have been used in HeLa cells imaging due to their low cytotoxicity and good biocompatibility (Fig. 15).

Moreover, some new functional groups can be introduced into the CDs by doping N and S elements, the emission wavelength of N, S co-doped CDs can be significantly red-shifted. Miao et al. [75] developed strong red emission N, S-CDs

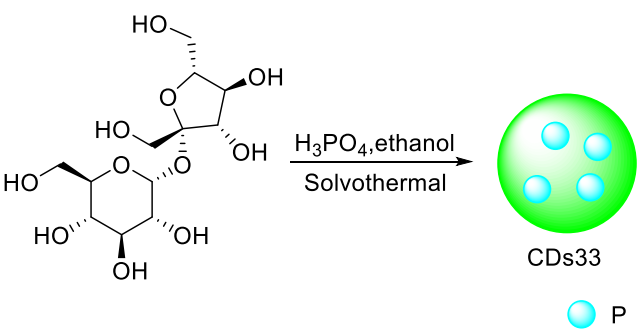

Fig. 33 Schematic presentation of CDs33 fabrication

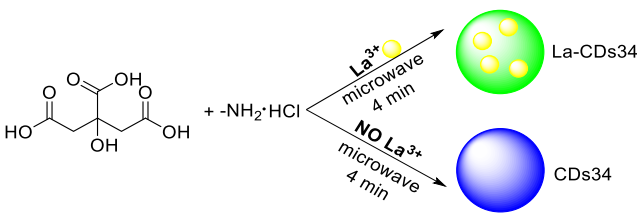

Fig. 34 Schematic presentation of CDs34 and La-CDs34 fabrication

Table 2 An overview on green-emitting carbon dots

Types	Particle composition	Particle Size(nm)	Ex/Em (nm)	QY (%)	Decay times(ns)	Ref
m-CDs28	C, H, O, N	1–5	400/530	11.43	3.525	[95]
e-CDs28	C, H, O, N	1–9	400/530	0.81	0.104	
CDs29	C, H, O, N	3.37	410/513	29	3.83	[96]
CDs30	C, H, O, N, P	2–4	390/510	30	–	[97]
CDs31	C, H, O, N	4.1	360/516	50	–	[98]
CDs32	C, H, O	4.5	420/538	–	–	[99]
CDs33	C, H, O, P	2–5	370/520	6	3.9	[100]
CDs34	C, H, O, N	2–6	360/445	10.21	10.34	[101]
La-CDs34	C, H, O, N, La	2–6	420/510	12.42	9.8	

(CDs16) using CA and thiourea as sources by a one-step hydrothermal route. Some new functional groups such as thiophene, pyrrole ring, and -SCN were introduced onto CDs16 by introducing S and N elements. Due to the conjugation of sp^2 carbon with thiophene and pyrrole units, the emission wavelength of CDs16 can be red-shifted. CDs16 showed sensitivity for Fe^{3+}. Doxorubicin was loaded onto CDs16 to form the CDs16-Dox, which was applied in fluorescence imaging of nude mice (Fig. 16).

Effects of other heteroatoms doped CDs

The type of heteroatom in the doped CDs is not limited to nitrogen and sulfur, and includes various elements such as phosphorus, boron, fluorine and selenium. Moreover, there is not only one heteroatom-doped CDs, but also a plurality of heteroatoms co-doped with CDs [76, 77]. The different types, positions and doping patterns of elements in CDs have different effects in modulating the color-emitting of CDs. Some can adjust the emission wavelength, and some can significantly improve the QY. Doping with heteroatoms greatly enhances PL emission of CDs, and the synergistic effect of co-doping facilitates the formation of band gaps, resulting in the high QY.

Patra et al. [78] synthesized nitrogen-containing CDs (N-CDs17), Phosphorus-doped CDs (P-CDs17) and Boron-doped CDs (B-CDs17) using CA, diethylenetriamine (DETA), o-phosphoric acid (o-PA) and boric acid (BA) by a hydrothermal method. The electron-rich P atom acts as an n-type donor to enhance the fluorescence properties of the CDs and contribute to the radiation transition pathway, while the electron-deficient B atom acts as a p-type dopant, which increases the non-radiative recombination pathway, resulting in a decrease in fluorescence. Therefore, the electron and hole transfer processes of n-type and p-type doping in CDs open up novel applications for a new generation of doped semiconductor materials (Fig. 17).

F-doping method can effectively modulate the color-emitting of CDs. Zuo et al. [79] used o-phenylenediamine or 1,2-diamino-4,5-difluorobenzene and tartaric acid through solvothermal method to obtain undoped CDs (CDs18) and F-doped CDs (F-CDs18). The former can emit fluorescence at 500 nm (480 nm excitation) or 550 nm (540 nm excitation), while the latter shows a large red-shifted fluorescence at 550 nm or 600 nm. The QY of CDs18 was 28%. After the F doped on CDs18, F-CDs18 showed higher QY of 31%. F-CDs18 can be used as a novel probe for efficient cell imaging of a variety of normal cells and cancer cells. In addition, F-CDs18 are also the Ag^+ detection probe which have been applied in environmental monitoring (Fig. 18).

The doped CDs show improved fluorescence and much higher QY than those of oxidized-CDs. Xie et al. [80] oxidized CNPs in Chinese ink and cut it into oxidized-CQDs, and then obtained Se-doped CDs (Se-CDs20) by reduction and in-situ doping reaction. Taking S and Se as examples, the electronegativity of the heterojunction may determine the emission wavelength of the doped CDs. Since the electronegativity of S and Se is smaller than C, it can be used as an electron acceptor, which causes the fluorescence emission peak of CDs to be red-shifted. The S element has a weak influence on the fluorescence position of CDs, while the Se-CDs20 can emit a noticeable

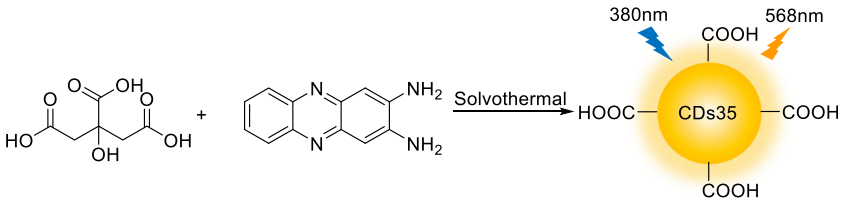

Fig. 35 Schematic presentation of CDs35 fabrication

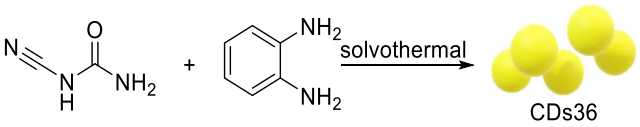

Fig. 36 Schematic presentation of CDs36 fabrication

yellow fluorescence. The yellow fluorescence of Se-CDs20 may be a special energy level from the formation of surface C-Se bonds. These doped CDs have a great potential in the development of various CDs-based functional materials and sensing devices (Fig. 19).

Effects of CDs associated with metal elements

Metal element doping can also modulate the color-emitting, QY and decay lifetime of CDs to some extent [81–84]. Yellow-emitting CDs (Mn-CDs20) have been synthesized using CA, urea, manganese acetate and toluene by Zhang et al. [85]. Compared with CDs20, Mn-CDs20 have an increase extent of conjugated π-domains and surface state, the emission wavelength was red-shifted. That is, Mn^{2+} can polymerize more CA molecules under dissolved heat conditions, thereby ensuring a high degree of conjugation of the sp^2-domain and the formation of more surface groups. The fluorescence QY and lifetime of CDs20 was 46% and 8.11 ns, respectively. Due to the Mn^{2+} doped on CDs20, Mn-CDs20 surface developed passivated defects, which showed higher QY (68.6%) and longer lifetime (8.75 ns). An ultraviolet-pumped LED was fabricated using Mn-CDs20. The LED displays warm orange light with a color purity of 99% (Fig. 20).

Wu et al. [86] synthesized Cu-CDs21 using Na_2[Cu (EDTA)] as raw material by one-step pyrolysis. Schiff-base-like structure transformed into a Cu coordination complex chelated with carbon matrixes. Cu-CDs21 showed copper content of 2.1%. Although Cu-CDs21 have no special performance in terms of fluorescence properties, their electron acceptor and donor capacities are 2.5 and 1.5 times higher than those of ordinary CDs. Cu-CDs21 have been used as photocatalysts for the photo-oxidation of 1,4- DHP in water solution (Fig. 21).

Cheng et al. [87] used zinc ions and CA as precursors to prepare strong yellow photoluminescence Zn^{2+}-doped CDs (Zn-CDs22) by solvothermal method. Compared with ordinary CDs22 synthesized without adding a zinc source, the addition of zinc causes the emission peak to shift from the blue band to the yellow band. Zinc exists in the form of Zn-O bonds, thereby promoting some kind of formation of defect states. The fluorescence QY and lifetime of CDs22 was 12% and 5.5 ns, respectively. Due to the Zn^{2+}-doped on Zn-CDs22, QY (51.2%) and decay lifetime (6.8 ns) is longer than that of CDs22. A bifunctional membrane was fabricated using colloidal PS-co-PMAA microspheres and Zn-CDs22. Zn-CDs22 have a good application prospect in the fields of inkjet printing, anti-counterfeiting, sensing and LED (Fig. 22).

Feng et al. [88] prepared a novel Co^{2+}-doped CDs (Co-CDs23) with an average size of 2.93 nm by hydrothermal method using 1-(2-pyridylazo)-2-naphthol and cobalt chloride as raw materials. The Co element introduces a new energy level for Co-CDs23, similar to charge transfer, resulting in orange fluorescence of Co-CDs23 with a QY of 6.2%. In the presence of Cr (VI), the interaction of Cr (VI) with the surface groups of Co-CDs23 produced an internal filter effect (IFE), which had potential for identifying Cr (VI) in real samples (Fig. 23).

In many CDs with metal elements, the forms of many elements are changed, which may be caused by the change of defect states caused by functional groups, or the new radiation transition caused by metal elements. In the future, only the strict, careful and thorough separation of metal element doped CDs can reveal the state of metal elements, indicating the fluorescence mechanism of metal doped CDs.

Throughout these existing reports, although people are trying to explore the mechanism of doping to improve the fluorescence characteristics of CDs, there is still no authoritative conclusion. Usually because of too many variables, it is difficult to accurately synthesize doped CDs with the desired fluorescence properties.

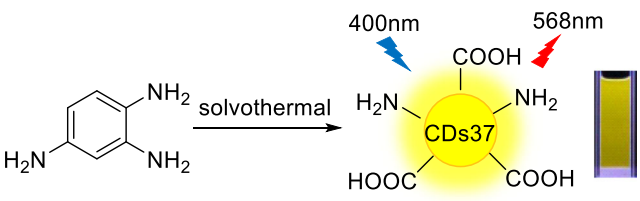

Fig. 37 Schematic presentation of CDs37 fabrication

Different color-emitting CDs

CDs have different color-emitting and can cover blue to red range, even ultraviolet and near infrared [57, 89, 90]. In recent years, many synthetic methods have been developed to prepare and optimize the optical properties of CDs. Systematic studies of different color-emitting CDs prepared by diverse precursors, methods and reaction conditions will help to clarify the factors affecting the fluorescence mechanism of CDs.

Blue light-emitting CDs

Although a variety of CDs have been reported, the most common is the blue light-emitting CDs. Most of these CDs showed strong fluorescence emission and high QY, but the Stokes shift was small and the photobleaching resistance was relatively poor.

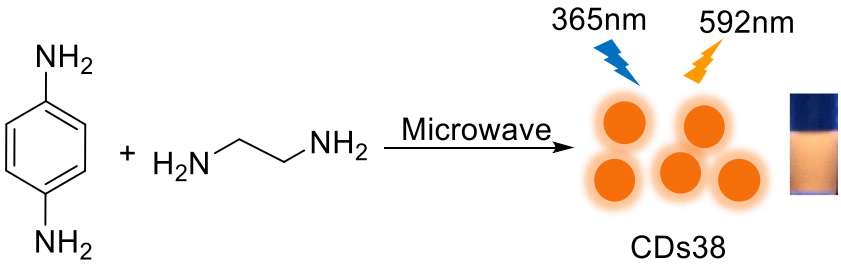

Fig. 38 Schematic presentation of CDs38 fabrication

Glutathione (GSH) containing free thiols, carboxyl and amine groups can form a protective shell around CDs. Wang et al. [91] synthesized blue-emitting CDs24 using glucose and GSH via a hydrothermal process. The QY of CDs24 in aqueous solution is 7.2%. The surface passivation of CDs24 resulted in their blue fluorescence emission. The surface state and size effect that affect the band gap of CDs24 are the cause of complex fluorescence behavior. CDs24 have great potential as novel luminescent thermometers and pH sensors, especially their fluorescence intensity is temperature sensitive and varies greatly over a temperature range from 15 to 60 °C (Fig. 24).

By doping N and S elements, the emission wavelength of N, S co-doped CDs can be significantly red-shifted. The heterocyclic aromatic structure of caffeine is a fusion of a pyrimidine ring and an imidazole ring, and is an effective precursor for the synthesis of CDs. Kim et al. [92] used caffeine, ammonium persulfate as raw materials to obtain o-CDs25 by a simple one-pot solid state synthesis method. The QY of o-CDs25 was 38%. When adding urea, u-CDs25 exhibited bright blue emission with a QY of up to 69%. CDs25 can establish a selective, sensitive fluorescence platform for detecting Ag^+ in aqueous media (Fig. 25).

The fluorescence enhancement may originate from polyaromatic structures induced by incorporated nitrogen atoms on CDs. Diamines can act as nitrogen precursors to form polyaromatic structures, resulting in stronger fluorescence emissions. Qian et al. [93] fabricated N-doped CDs (CDs26) through a solvothermal approach using CCl_4 and diamines. CDs26 emit bright blue fluorescence and the QY is greatly elevated to 36.3% due to the introduction of N atoms. The average fluorescence lifetime of CDs26 was 10.3 ns. The pyridinic and pyrrolic N atoms can be regarded as defect structures, the emergence of these defects would lead to formation of more polyaromatic structures and give rise to stronger emission. CDs26 can be used as a multi-function sensor for the detection of pH, Ag^+, $Fe^{3+}$and H_2O_2 in aqueous solution. The fluorescence intensity of CDs26 is inversely proportional to the pH value, ranging from 5.0 to 13.5. In addition, CDs26 can be applied to human Hela cells imaging (Fig. 26).

Metal element doping can also modulate the color-emitting and QY of CDs by chelation enhanced fluorescence mechanism. Lin et al. [94] prepared N, P-CDs (CDs27) using o-phosphorylethanolamine and CA as precursors via hydrothermal treatment. CDs27 with blue-green emission had a maximum emission wavelength at 435 nm when the excitation was 325 nm. CDs27 with QY of 8.17% showed excitation-dependent emission. CDs27 exhibited a fluorescence enhancement effect in the presence of Cd^{2+} from 0.5–12.5 μM with a LOD of 0.16 μM. The phenomenon may be attributed to chelation enhanced fluorescence mechanism via the coordination reaction between functional groups on the surface and Cd^{2+}. The method has been used as a nanoprobe for detection of Cd^{2+} in serum and urine samples (Fig. 27 and Table 1).

Green light-emitting CDs

Green light-emitting CDs are also more common in recent years, but have lower QYs than blue light-emitting CDs. It is still a challenge to prepare highly stable water-soluble green light-emitting CDs.

Different surface functional groups will effectively modulate the color-emitting of CDs. CDs with different optical properties can be prepared by different synthesis methods. Wang et al. [95] prepared microwave-synthesized CDs (m-CDs28) by microwave method using CA and urea as precursors. The electrochemical-synthesized CDs (e-CDs28) were prepared by using graphite rod as carbon source. Ultrafast spectroscopy reveals that a particular edge state consisting of

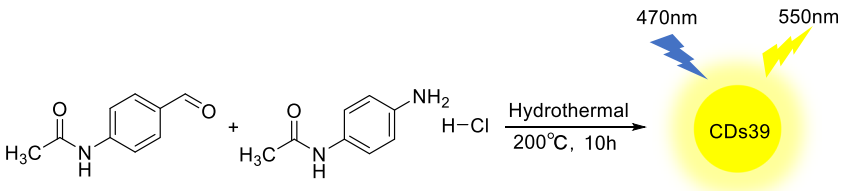

Fig. 39 Schematic presentation of CDs39 fabrication

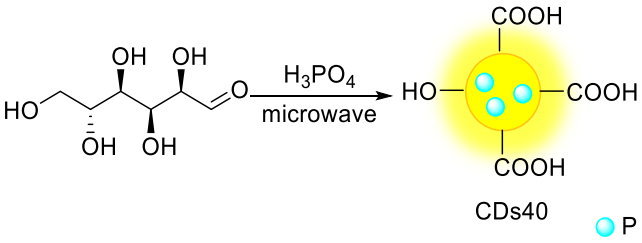

Fig. 40 Schematic presentation of CDs40 fabrication

several carbon atoms at the edge of the carbon skeleton and chemical groups with C=O is the origin of green emissions. The optical properties of CDs are mainly determined by the competition between different emission centers and traps (Fig. 28).

The surface states can capture the excited state energy, resulting in a significant red shift in the emission wavelength of CDs. Yang et al. [96] synthesized green light-emitting CDs29 by hydrothermal treatment of ethylene diamine in the presence of phenol. The fluorescence QY and lifetime of CDs29 was 15% and 3.83 ns, respectively. CDs29 showed a maximal emission wavelength at 513 nm under 410 nm excitation. The green emission of CDs29 was attributed to the capture of excited state energy by surface states. A fluorescence method for the insecticide cartap quantitation was developed by using green fluorescence CDs29 and Au NPs based on IFE. The method was used for the detection of cartap in the 5–300 nM with a detection limit of 3.84 nM (Fig. 29).

Polyethyleneimine (PEI) is an amino-rich cationic polyelectrolyte to prepare fluorescence CDs. However, high molecular weight PEI is more toxic than low molecular weight oligoethylenimine (OEI). Zheng et al. [97] synthesized green fluorescence CDs30 through carbonization of OEI and β-cyclodextrin (βCD) via a heating process in phosphoric acid. The QY of CDs30 is 30%. CDs30 containing carboxyl and carbonyl groups are doped with nitrogen and phosphorus. CDs30 have been used in biomedical fields such as cell labeling and imaging. In addition, the cytotoxicity of Dox-loaded CDs30 nanocomposites on H1299 cancer cells was enhanced compared with that of free Dox (Fig. 30).

Active dry yeast (ADY) contains a variety of carbon compounds such as amino acids, nucleotides, sugars and vitamins, which can be used as a precursor for large-scale synthesis of CDs. Folic acid (FA) has high affinity and stability and is an ideal ligand for Folate receptor (FR), an important tumor biomarker. Zhang et al. [98] used ADY as a raw material to prepare bright green light-emitting CDs31 by simple and rapid microwave method. Folic acid- conjugated CDs (FA-CDs31) were further prepared by covalent coupling of CDs31 and FA by EDC/NHS reaction. The surface of CDs31 has abundant -OH, -COOH and -NH_2 groups and self-passivation of surface traps. FA-CDs31 can be used for targeting and imaging of FR-positive cancer cells. FA-CDs31 have broad prospects for cancer diagnosis and treatment (Fig. 31).

Different surface functional groups will facilitate the color-emitting modulation of CDs. Mohan et al. [99] fabricated fluorescent CDs32 using ascorbic acid via hydrothermal method in the presence of ethylene glycol. CDs32 emit wavelengths of 382 nm and 538 nm under excitation of 320 nm and 420 nm, respectively. Under 365 nm excitation, CDs32 exhibit dual-band emission, one at 435 nm and the other at 538 nm. The green fluorescence of CDs32 is attribute to the formation of molecular states including C=O and -COOH on the surface of CDs32. The blue fluorescence is attribute to all kinds of surface states of CDs32 including both mono- and double-bonded oxygen chemical groups. CDs32 have potential application prospects in cell imaging (Fig. 32).

The doped of phosphorus as a heteroatom into CDs can produce new optical properties. Jiang et al. [100] used sucrose as carbon source to prepare green light-emitting CDs33 via a solvothermal process. CDs33 with a QY of 6% exhibited stable green fluorescence at 520 nm. CDs33 with good reproducibility have a reversible linear response to temperature from 20 to 85 °C as well as the temperature resolution better than 0.5 °C. The green fluorescence of CDs33 can be attributed to the modulation of chemical and electronic properties caused by the introduction of P atoms. Moreover, CDs33 have potential as a fluorescent probe for temperature monitoring and cell imaging (Fig. 33).

Fig. 41 Schematic presentation of CDs41 fabrication

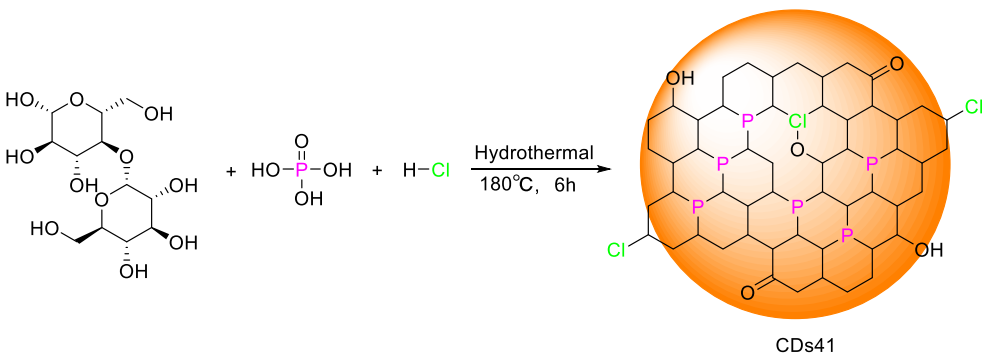

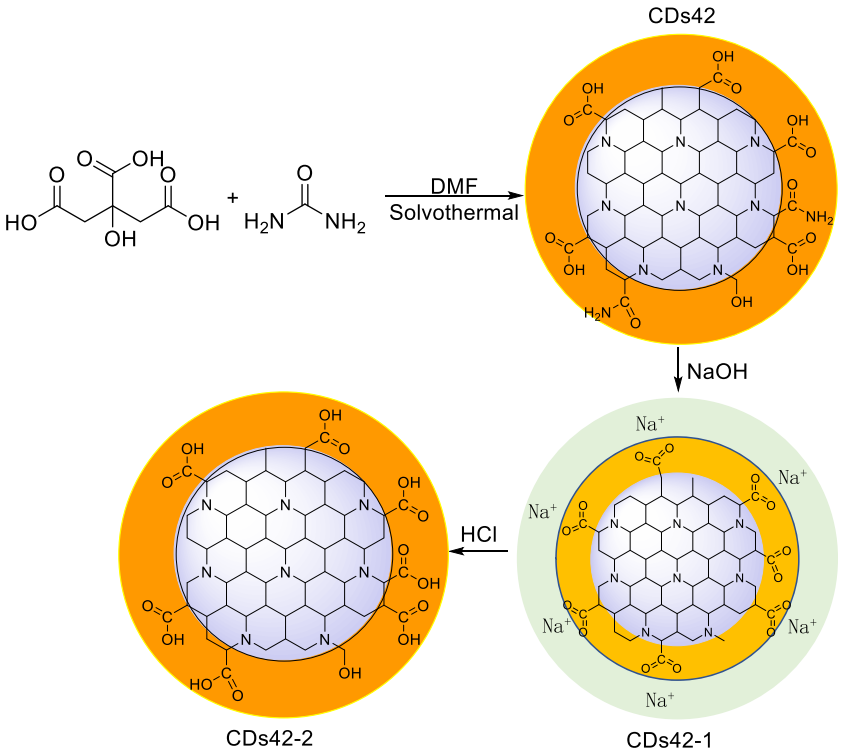

Fig. 42 Schematic presentation of CDs42, CDs42–1 and CDs42–2 fabrication

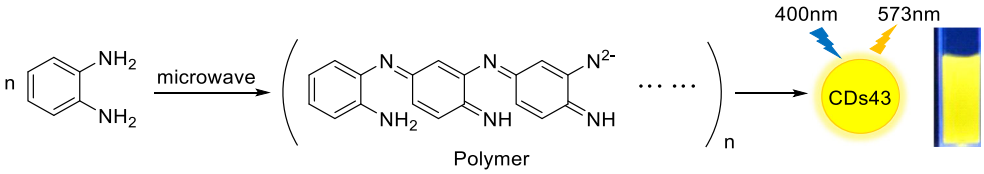

Fig. 43 Schematic presentation of CDs43 fabrication

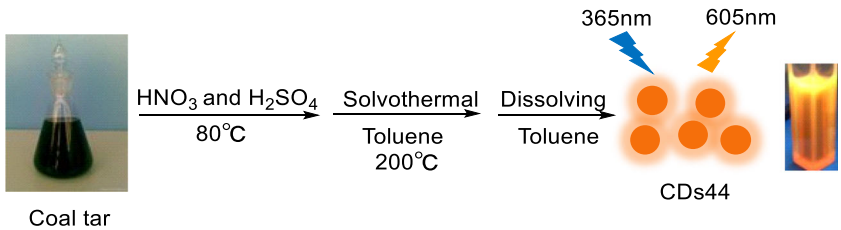

Fig. 44 Schematic presentation of CDs44 fabrication

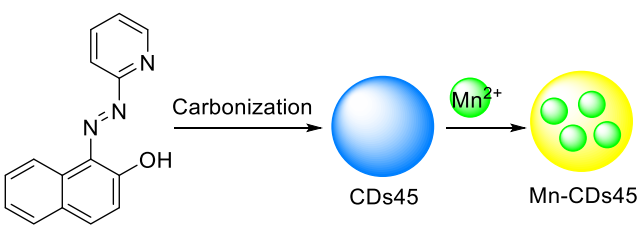

Fig. 45 Schematic presentation of CDs45 and Mn-CDs45 fabrication

Table 3 An overview on yellow-emitting carbon dots

Types	Particle composition	Particle Size(nm)	Ex/Em (nm)	QY (%)	Decay times(ns)	Ref
CDs19	C, H, O, N, Se	2–6	408/563	11	3.27	[80]
CDs23	C, H, O, N, Co	2.93	485/564	6.2	–	[88]
CDs35	C, H, O, N	5.5–9	380/568	24	–	[104]
CDs36	C, H, O, N	2.4–5.9	420/556	19	4.39	[105]
CDs37	C, H, O, N	14.3	400/568	32.5	1.87	[106]
CDs38	C, H, O, N	3–6	365/592	14	3.16	[107]
CDs39	C, H, O, N	1.75–4.25	470/550	–	–	[108]
CDs40	C, H, O, N, P	4.5–13.5	363/560	11.5	0.91	[109]
CDs41	C, H, O, P, Cl	4.83	390/590	14.9	–	[110]
CDs42–1	C, H, O, N, Na	4–10	540/580	46	3.8	[111]
CDs42–2	C, H, O, N	4–10	540/590	6	3.8	
CDs43	C, H, O, N	8–11	400/573	38.5	2	[112]
CDs44	C, H, O, N	1.5–4.5	365/605	29.7	–	[113]
Mn-CDs45	C, H, O, N, Mn	4.72	365/565	4.7	2.56	[114]

Rare-earth elements have special properties due to their unique atomic structure. It can be used as a heteroatom for the preparation of co-doped CDs, thereby improving the optical properties of the original CDs. Yang et al. [101] fabricated La-doped CDs (La-CDs34) that the emission shifted from blue to green (445 to 510 nm) by microwave pyrolysis. The QY of CDs34 and La-CDs34 was 10.21% and 12.42%, respectively. The fluorescence lifetime of CDs34 and La-CDs34 was 10.34 ns and 9.8 ns, respectively. The fluorescence enhancement of La-CDs34 may be caused by local structural changes caused by La-O bonds. Since La^{3+} do not bind to surface oxygen atoms, but combine with oxygen atoms inside La-CDs34, which promotes electron or hole distribution, increases charge transfer and reduces the energy gap. The combined effect enhances the PL performance of La-CDs34. La-CDs33 were successfully used for sensitive imaging of Fe^{3+}, and the LOD was 91 nM in live HeLa cells (Fig. 34 and Table 2).

Yellow light-emitting CDs

The common photodamage of biological substrates by autofluorescence and short-wavelength excitation light limits the biological application of blue and green light-emitting CDs [102, 103]. Currently, yellow light-emitting CDs with large Stokes shifts have been prepared, but QYs are generally low. The preparation of yellow light-emitting CDs with high QYs typically relies on the use of specific precursors in special solvents, these CDs exhibit high ability in biological applications.

The emission colors can be adjusted by changing the surface states of CDs. The 2,3- phenylenediamine (PD) with larger conjugated structure is favorable for the preparation long-wavelength emission CDs. Based on it, our groups developed yellow light-emitting CDs35 via solvothermal method using CA and PD as the precursors [104]. CDs35 showed a fluorescence QY of 24% and a stokes shift of 188 nm. The fluorescence emission peak centered at 568 nm under the excitation of 380 nm. Due to the high oxidation degree of -COOH on CDs35 surface, the energy band gap is reduced, leading in yellow light-emitting. CDs35 has been applied to the detection of Ag^{+} and GSH in living cells, and will be further applied in environmental monitoring and biomedicine (Fig. 35).

Dicyandiamide is an excellent N-containing precursor for the preparation of CDs. Li et al. [105] synthesized green-yellow light-emitting N-doped CDs (CDs36) using dicyandiamide and 1,2 -diaminobenzene as the precursors by one-pot hydrothermal process. The optimal excitation and emission wavelength are at 420 and 556 nm. CDs36 in

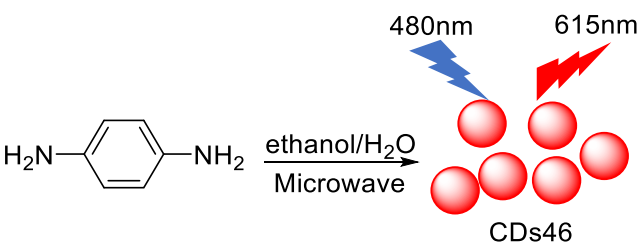

Fig. 46 Schematic presentation of CDs46 fabrication

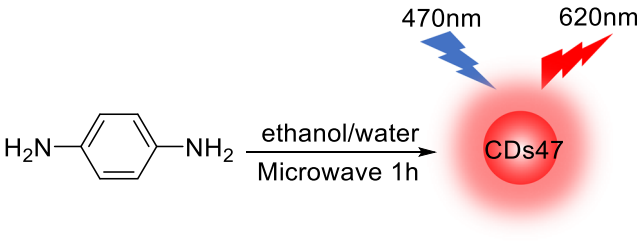

Fig. 47 Schematic presentation of CDs47 fabrication

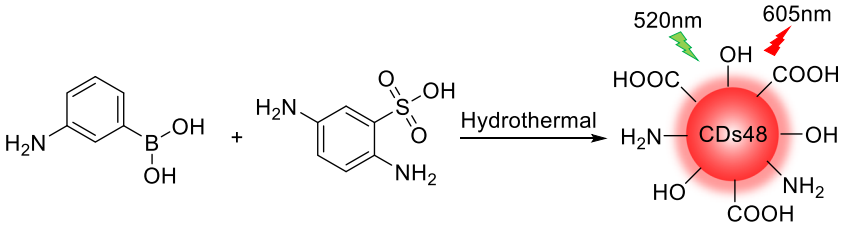

Fig. 48 Schematic presentation of CDs48 fabrication

aqueous solution have two typical UV-visible absorption peaks at 276 nm and 360 nm. The transition at 360 nm is due to the trapping of excited state energy by the surface states, resulting in strong emission. CDs36 can measure Ag^+ with a LOD of 5×10^{-8} mol L^{-1} in water and have potential applications for imaging HepG2 cells (Fig. 36).

Bright yellow N-doped CDs (CDs37) with the emission maximum at 568 nm were prepared using 1,2,4-triaminobenzene as carbon precursors via a solvothermal reaction by Jiang et al. [106] The QYs were 32.5% in ethanol. There is only one dominant emission state in CDs37, and the -COOH groups and/or C-N related structures in CDs37 are responsible for the yellow light-emitting. CDs37 and Ag^+ can be used to detect cysteine in human plasma samples, which has potential application prospects in the cellular imaging and bifunctional sensing (Fig. 37).

Nitrogen atoms on CDs surface will provide lone pairs of electrons, leading to Fermi level shift, band gap and optical properties change. Ding et al. [107] prepared the N-doped CDs (CDs38) with bright orange fluorescence emission at 592 nm using p-phenylenediamine as the precursor by microwave method. The prepared CDs38 show excitation wavelength independence and sensitive pH response. The optimal excitation and emission wavelength were at 535 nm and 592 nm, respectively. The surface of CDs38 have -OH and -NH_2 groups. Furthermore, CDs38 has been successfully used as a fluorescent probe for A-549 cell imaging and has potential application prospects in the detection of pH in living cells (Fig. 38).

Bandgap transitions of conjugated π-domains and surface defect states can jointly modulate the color-emitting of CDs. Mutuyimana et al. [108] synthesized yellow light-emitting CDs39 using 4-acetamidobenzaldehyde and 4-aminoacetenilide hydrochloride via hydrothermal process. CDs39 showed a maximum emissive wavelength at 550 nm under 470 nm excitation. The yellow fluorescence of CDs39 derived from the bandgap transitions of conjugated π-domains and/or surface defect states. The fluorescence of CDs39 was quenched by Cr^{5+} via static quenching effect. CDs39 were used as a fluorescent nanoprobe for the determination to Cr^{5+} in the range of 1–400 μM with a LOD of 0.13 μM. This method was successfully applied to the detection of Cr^{5+} in water and biological tissue samples (Fig. 39).

Based on the bandgap of conjugated π-domains and surface states mechanism, Xu et al. [109] prepared yellow light-emitting CDs (CDs40) using glucose and H_3PO_4 via microwave method. The amphibious CDs40 show strong yellow fluorescence in both water and organic solvents. The surface of CDs40 has oxygen-containing and phosphorus-containing functional groups. The degree of oxygen-containing groups and the size of the particles can tune the emission wavelength of CDs40. Furthermore, CDs40 can detect chromium by fluorescence colorimetry, and the LOD of Cr (VI) ions is 0.02×10^{-6} M. It has broad prospects in practical applications such as bio-imaging, optical equipment and Cr (VI) visual field nanoprobe (Fig. 40).

Co-doping of P and Cl can facilitate the formation of band gaps and enhanced fluorescence emission of CDs41. Wang et al. [110] prepared P, Cl-CDs (CDs41) via one-pot hydrothermal treatment using maltose, phosphoric acid and hydrochloric acid as C, P, and Cl sources, respectively. CDs41 exhibited yellow fluorescence with a QY of 14.9%. They have excitation/emission maxima at 390/590 nm. The fluorescence of CDs41 were quenched by Fe^{3+} due to their strong coordination with Fe^{3+}. This fluorescence nanoprobe was successfully applied to the determination of Fe^{3+} in water and human serum samples in the range from 0.1–8.0 μM, and the detection limit is 60 nM (Fig. 41).

By conjugated sp^2-domain controlling and surface charges engineering, Qu et al. [111] developed high-efficiency orange-emitting CDs42 by solvothermal pathway with CA and urea as precursors. DMF is a good solvent for the formation of

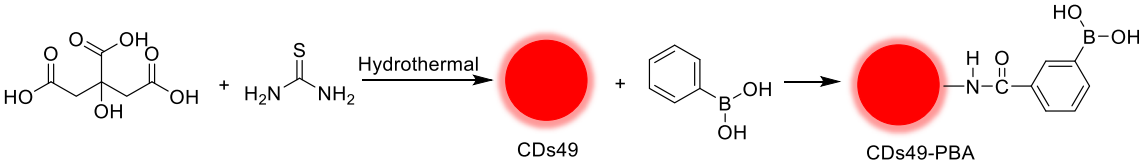

Fig. 49 Schematic presentation of CDs49 and CDs49-PBA fabrication

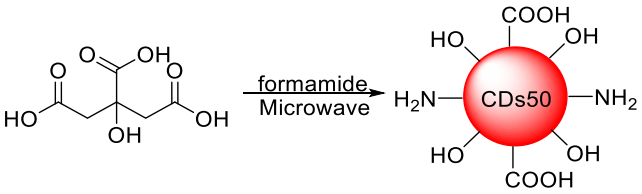

Fig. 50 Schematic presentation of CDs50 fabrication

CDs42 with large conjugated sp^2 domains and is the basis for orange bandgap emission. The emission of CDs42–1 and CDs42–2 were centered at 580 nm and 590 nm under 540 nm excitation, with QYs of 46% and 6%. The surface metal ion-functionalization increased the carboxylate groups on the inner surface of CDs42–1, leading to an electron-rich property. The orange emission of CDs42–1 and CDs42–2 are bandgap emission of the conjugated sp^2 domain in the nitrogen-rich multilayer graphene-like core. A highly efficient orange emissive starch/CDs42–1 phosphor (QY of 21%) was prepared, and warm WLEDs were realized using only green and orange emissive starch/ CDs42 phosphors (Fig. 42).

Phenylenediamines having three isomers of o-phenylenediamine, m-phenylenediamine and p-phenylenediamine are excellent precursors for the preparation of CDs. Song et al. [112] prepared CDs43 with strong yellow fluorescence by microwave-assisted method using o-phenylenediamine as the carbon precursor. The emission peak of CDs43 solution was centered at 573 nm under 400 nm excitation, and the QY is 38.5%. The fluorescence behavior of CDs43 is attributed to differences in the molecular structure of the phenylenediamine isomers that might form CDs43 with different morphology, size, or chemical groups. CDs43 can be used for fluorescence imaging of SW480 cells and detection of Fe^{3+} and H_2O_2, the LOD for Fe^{3+} and H_2O_2 is 16.1 nM and 28.1 nM, respectively (Fig. 43).

Coal tar is a cheap and abundant by-product containing polycyclic and heterocyclic aromatic molecules. Geng et al. [113] used coal tar to nitrate and then toluene solvent heat treatment to synthesize orange fluorescent CDs44. The QYs of CDs44 in the toluene solution was 29.7%. The orange-emitting CDs44 exhibit excitation wavelength dependence. As the excitation wavelength increases, larger sized CDs44 can be excited and emit fluorescence at long wavelengths, resulting in the red-shift of emission wavelength. In addition to size effects, the distribution of different emission sites on CDs44 may also cause the redshift. The PEGylated liposomes encapsulating CDs44 are useful for bioimaging. Liposomes-CDs44b have been successfully used in vitro and in vivo imaging (Fig. 44).

Metal element doping may affect surface defect states fluorescence, making bandgap transitions of conjugated π-domains modulate the color-emitting of CDs. Feng et al. [114] successfully synthesized manganese-doped CDs (Mn-CDs45) using 1-(2-pyridylazo)-2-naphthol as both a carbon source and a metal ion chelating agent. The addition of Mn^{2+} changes CDs from the original blue fluorescence to yellow fluorescence. The blue fluorescence in CDs comes from the surface defect state, while the yellow fluorescence is caused by the bandgap transitions of conjugated π-domains. That is to say, the change of the fluorescence position is not because the Mn element induces a new energy level, but Mn^{2+} annihilates the surface defect state luminescence by binding with the N atom in the defect, so that the bandgap transitions of conjugated π-domains becomes dominant. In addition, Mn-CDs45 have been applied in bioimaging, fluorescent inks, nanoprobe and fluorescent films (Fig. 45 and Table 3).

Red light-emitting CDs

Red light-emitting CDs shows optimal tissue penetration, minimal damage to biological samples, and low background interference [115]. In addition, red CDs can provide missing building blocks for full-color emission spectroscopy, for

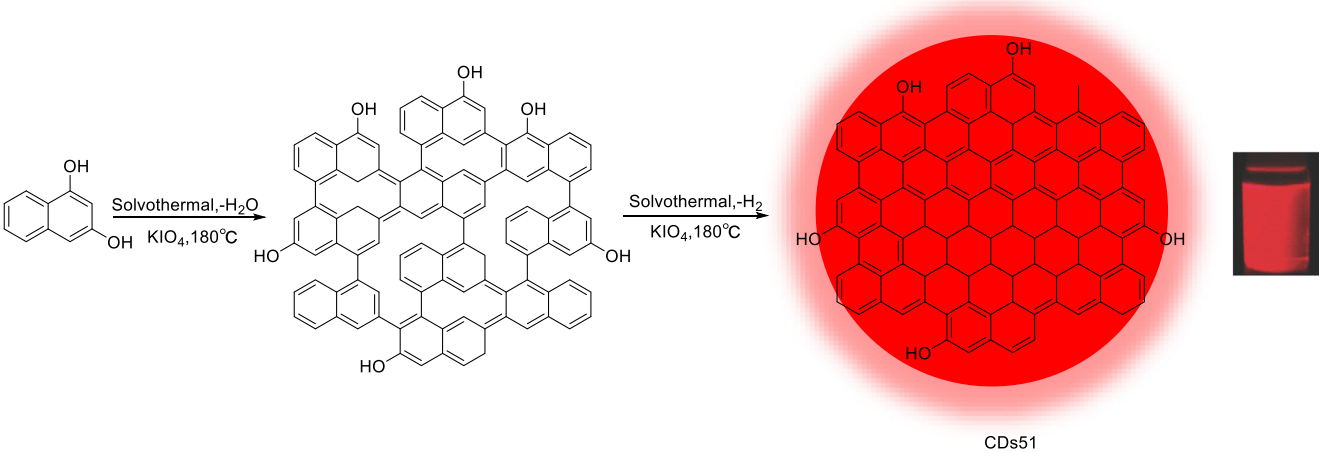

Fig. 51 Schematic presentation of CDs51 fabrication

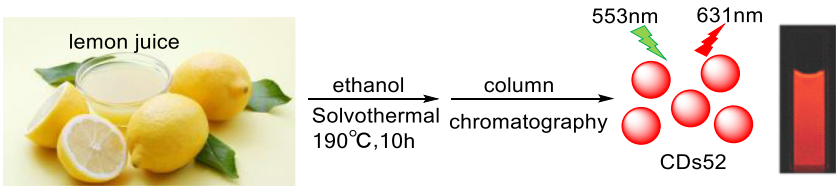

Fig. 52 Schematic presentation of CDs52 fabrication

example, white light emitting diodes. Therefore, the development and promotion of long-wavelength emission CDs are of great significance in the field of lighting and biomedical. Currently, The QYs of red light-emitting CDs are generally low. In order to improve the fluorescence behaviors of red CDs, a large number of studies including the selection of the reaction precursors and optimization of the synthetic approach have been continuously conducted.

N-doping is a facile and effective way to improve the optical properties of CDs. Wang et al. [17] prepared red light-emitting CDs46 with maximum emission wavelength 615 nm by a microwave-assisted method using p-phenylenediamine as the precursor. The PL QY of CDs46 was 15%. CDs46 were successfully applied as the fluorescent probe for the detection of glutathione (GSH). Furthermore, CDs46 based turn-on fluorescent nanothermometry have potential applications in living cell imaging and temperature sensing (Fig. 46).

Under the same synthesis conditions, Sun et al. [116] fabricated red light-emitting CDs47 by one-step microwave-assisted method using p-phenylenediamine as carbon and nitrogen source. The PL QY of CDs47 was 15%. CDs47 had a maximum emission wavelength at 620 nm when the excitation was 470 nm. The excitation-independent FL behavior suggested that the FL properties of CDs47 are mostly dependent on the surface states. Additionally, CDs47 were used as a nanoprobe for detection of pH and Fe^{3+} in aqueous solution and *E. coli* bacteria cell, simultaneously. The LOD for Fe^{3+} is 15 nM in the 0 to 30 μM range (Fig. 47).

Co-doping of N, B and S atoms enables CDs to exhibit excellent optical properties, good biocompatibility and low cytotoxicity. Huang et al. [117] synthesized NBS-CDs (CDs48) by a one-step hydrothermal method by using 3-aminobenzeneboronic acid and 2,5-diaminobenzenesulfonic acid as precursors. The maximum excitation and emission wavelength of CDs48 are 520 nm and 605 nm, respectively.

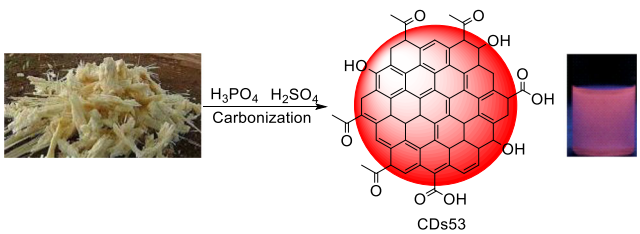

Fig. 53 Schematic presentation of CDs53 fabrication

CDs48 shows an excitation wavelength-independent feature. Some related functional groups (-OH, -COOH, and $-NH_2$) are existed on the surface of CDs48. The doping of N, B, and S atoms can result in the relative uniform size distribution and surface state of CDs48. Furthermore, red light-emitting CDs48 were used for the detections of Ag^+ and L-cysteine with detection limits as low as 0.35 mM and 0.045 mM, respectively (Fig. 48).

Phenylboronic acid (PBA) might be used as a mediator to shorten the contact time between CDs and cells, which is conducive to the applications of CDs in the field of bioprobes. Li et al. [118] fabricated red light-emitting N, S co-doped CDs (CDs49) using CA and thiourea via a hydrothermal method. After coupling with PBA, CDs49-PBA was synthesized. At 550 nm excitation, the maximum emission wavelength is 593 nm. The PL QY in water was 23%. After doping the heteroatoms S and N, the excitation and emission wavelengths of CDs49 show a significant red shift. The surface of CDs49 contains $-NH_2$, -COOH, -SCN and -OH groups. CDs49-PBA show high sensitivity to Fe^{3+} and are expected to be used as an effective detection platform for other biological samples and environmental systems (Fig. 49).

Formamide containing carbonyl and amino groups plays a key role in the successful preparation of long-wavelength red emission CDs. Sun et al. [119] prepared red light-emitting CDs50 by one-step microwave assisted heating of CA formamide solution. The PL QY of CDs50 was 22.9%. CDs50 were composed of rich amino and hydroxyl functional groups. Moreover, CDs50 can selectively stain RNA-rich nucleolus and had been successfully applied to photothermal cancer therapy in vitro (Fig. 50).

One molecule of 1,3-dihydroxynaphthalene can as the smallest sp^2 domain with -OH groups. Under the strong oxidation of KIO_4, this domain can form large conjugated sp^2 clusters with -OH groups. Wang et al. [120] have devised a DCDP(dehydrative condensation and dehydrogenative planarizationmethod) using 1,3-dihydroxynaphthalen as carbon source to synthesize CDs51. The QY of red light-emitting CDs51 was up to 53%. In the decoupled DCDP route, DC enables size tuning while DP ensures a high degree of π-conjugation. CDs51 are a conjugated sp^2 cluster of uniform size with -OH groups at the edges, producing a strong red emission. For the first time, an UV-pumped CDs51 phosphors-based warm WLED was prepared with a color rendering index of 97 (Fig. 51).

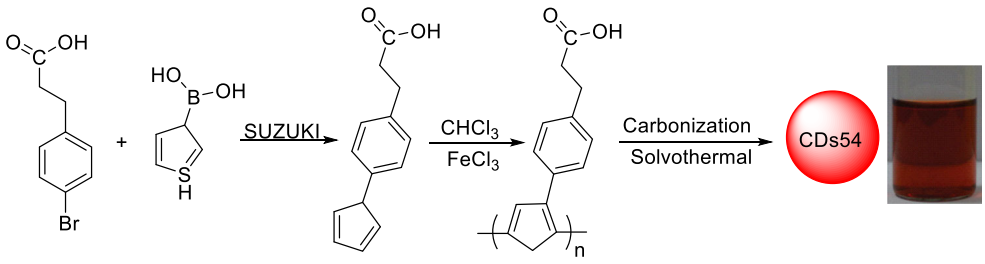

Fig. 54 Schematic presentation of CDs54 fabrication

Biomass CDs with superior optical properties and low cytotoxicity can reduce resource waste and realize sustainable development. Ding et al. [121] synthesized high-efficiency red light-emitting CDs52 by solvothermal method using lemon juice. The obtained CDs52 with a QY of 28% were monodisperse with an average diameter of 4.6 nm, and exhibited excitation-independent emission at 631 nm. The surface state of CDs52 and the nitrogen-derived structure in the CDs52 core synergistically caused intense red fluorescence. The low cost, ecologically friendly synthesis method and good optical properties make CDs52 have great application value in the field of biological imaging and optoelectronics (Fig. 52).

Bagasse is a kind of natural raw material for the preparation of biomass CDs. Jiang et al. [122] prepared red light-emitting CDs53 by one-step carbonization of bagasse with H_2SO_4 and H_3PO_4 at 100 °C. CDs53 are mainly composed of sp^2 graphitized carbon atoms with a small amount of sp^3 carbon defects. The water-dispersed CDs53 are sulfur-doped and rich in -COOH on the surface. The polyvinylidene fluoride-loaded CDs53 can selectively detect gaseous ammonia with a low detection limit, which can meet the sensitive monitoring of toxic ammonia pollution (Fig. 53).

Polymers such as polythiophene phenylpropionic acid (PPA) have a larger conjugated structure and can be used as a precursor to prepare novel CDs. Ge et al. [123] fabricated CDs54 using PPA as the precursor. CDs54 showed red light-emitting from 500 to 800 nm with a peak at 640 nm. The red-emitting CDs54 exhibited a photothermal conversion efficiency of up to 38.5% under 671 nm laser irradiation. CDs54 were carboxylate-terminated and sulfur-doped with an average size of 10 nm. what' more, CDs54 can be used as active agents in fluorescent, photoacoustic, and thermal theranostics in living mice (Fig. 54 and Table 4).

Multicolor-emitting CDs

Obtaining the fluorescence emission of the entire visible spectrum is considered to be a key requirement for the successful implementation of CDs in almost all practical applications [115, 124, 125]. Although many reports have proposed fluorescence-related emission, the relative wavelength shift often does not cover the entire visible spectrum, the fluorescence emission intensity is significantly reduced. Such optical displacements cannot be truly marked as tunable. What is really needed is a method of changing the chemical and physical properties of CDs to modulate the color-emitting of CDs without affecting the peak emission intensity [31, 126–128]. The multicolor emission of CDs is primarily derived from different surface states.

Table 4 An overview on red-emitting carbon dots

Types	Particle composition	Particle Size (nm)	Ex/Em (nm)	QY (%)	Decay times(ns)	Ref
CD6	C, H, O, N, S	4.5	440/590	15	1.2	[46]
CDs16	C, H, O, N, S	4.42	560/594	29	12.9	[75]
CDs46	C, H, O, N	2.2–6.5	480/615	15	–	[17]
CDs47	C, H, O, N	3.8	470/620	15	–	[116]
CDs48	C, H, O, N, S, B	1.5–4	520/605	11.6	1.35	[117]
CDs49	C, H, O, N, S	–	330/471	–	–	[118]
CDs49-PBA	C, H, O, N, S, B	3.27	550/593	23	6.15	
CDs50	C, H, O, N	2.5–5.5	540/640	22.9	–	[119]
CDs51	C, H, O	5	530/628	53	10.8	[120]
CDs52	C, H, O, N	4.6	553/631	28		[121]
CDs53	C, H, O, N	3.6	372/630	–	–	[122]
CDs54	C, H, O, S	10 ± 4	543/640	2.3	–	[123]

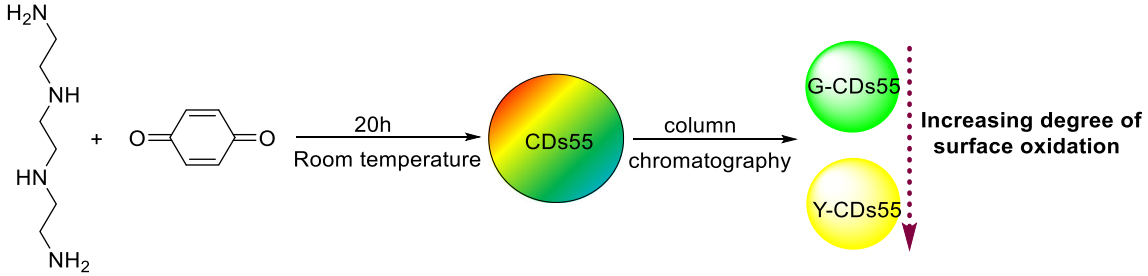

Fig. 55 Schematic presentation of CDs55, G-CDs55 and Y-CDs55 fabrication and its fluorescence mechanism

Different surface oxidation degree will facilitate the color-emitting modulation of CDs. CDs55 with a QY of up to 35.3% were synthesized by Schiff base reaction using triethylenetetramine (TETA) and p-benzoquinone [129]. CDs55 can be further separated into green G-CDs55 and yellow Y-CDs55 through a silica gel column. The QYs are 35.3% and 17.5%, respectively. G-CDs55 show an excitation-independent feature but Y-CDs55 are excitation-dependent. G-CDs55 have a higher surface oxidation degree than Y-CDs55, resulting in red-shifted emission from 558 nm to 543 nm, which can be attributed to the reduction of band gap. Moreover, Y-CDs55 with good photostability can be widely used in cell imaging and analysis, while G-CDs55 are easier to be photobleached (Fig. 55).

The solvents can adjust the dehydration and carbonization of precursors, which then vary oxygen-containing functional groups on CDs surface, resulting in different optical properties of CDs. Hu et al. [130] mixed CA or ethylene glycol (EG) with ethylenediamine endcapped polyethylenimine (PEI-EC), and added a dehydrating agent (H_3PO_4) or a reducing agent ($NaBH_4$) to prepare tunable fluorescence emission CDs56 from blue (400 nm) to NIR (710 nm). CDs56 rich in -COOH on the surface mainly emit blue fluorescence. As the CO-C or C-O in CDs increases, the band gap of surface states of CDs56 gradually decreases, resulting in the red-shift of emission wavelength. CDs56 can be widely used in lighting and biosensing (Fig. 56).

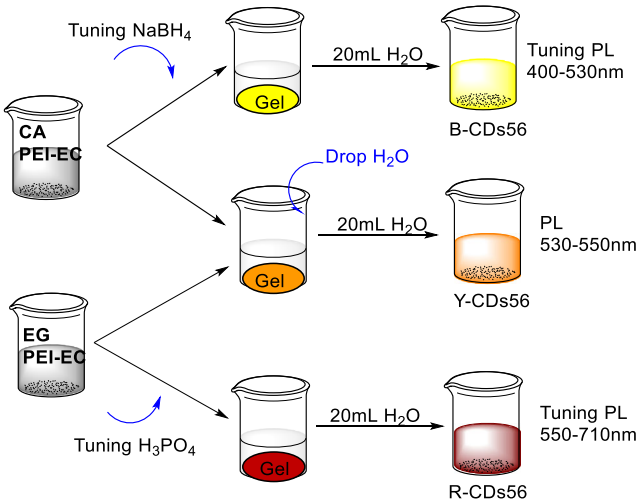

Fig. 56 Schematic presentation of CDs56 fabrication

Controlling surface -NH_2 groups density by varying the reaction temperature is a facile way to modulate the color-emitting, QY and decay lifetime of CDs. CDs57 were synthesized by using CA and urea as precursors via hydrothermal method [131]. CDs57 prepared at 240 and 160 °C have excitation-dependent and excitation-independent fluorescence, respectively. CDs57–1 prepared at lower temperatures have a higher density of -NH_2 groups on their surface, which results in the band gap narrowed, further leading to the redshift of emission and higher QY (44.7%) and longer lifetime (7.13 ns). The fluorescence QY and lifetime of CDs57–2 was 20.8% and 5.21 ns, respectively. CDs57 have been used to fabricate multicolor CDs57/polymer composites, which have potential applications in the field of LED. In addition, CDs57 can also be used as probes for the detection of Be^{2+}.The detection limit was 23 μM (Fig. 57).

Controlling surface states using C=N functional groups is an effective way to modulate the color-emitting of CDs. Han et al. [127] fabricated multicolor-emitting CDs58 using hydroquinone and EDA via hydrothermal method. CDs58 were separated via column chromatography and showed bright yellow, green, and blue fluorescence. The multicolor emission of CDs58 was primarily connected with the C=N functional groups on the surface. The band gap decreased with increasing content of C=N, resulting in the red shift of the fluorescence emission. Moreover, CDs58 exhibited stable fluorescence emission and excellent water solubility, these properties promoted their application in fluorescent ink and pH sensing (Fig. 58).

The -COOH and -NH_2 groups can modulate the color-emitting of CDs by electron transfer according to the electron absorption and electron donation behavior of chemical groups. Dhenadhayalan et al. [132] used CA and EDA as precursors to synthesize carboxyl and amine functionalized CDs (B-CDs59 and G-CDs59) by microwave method. The

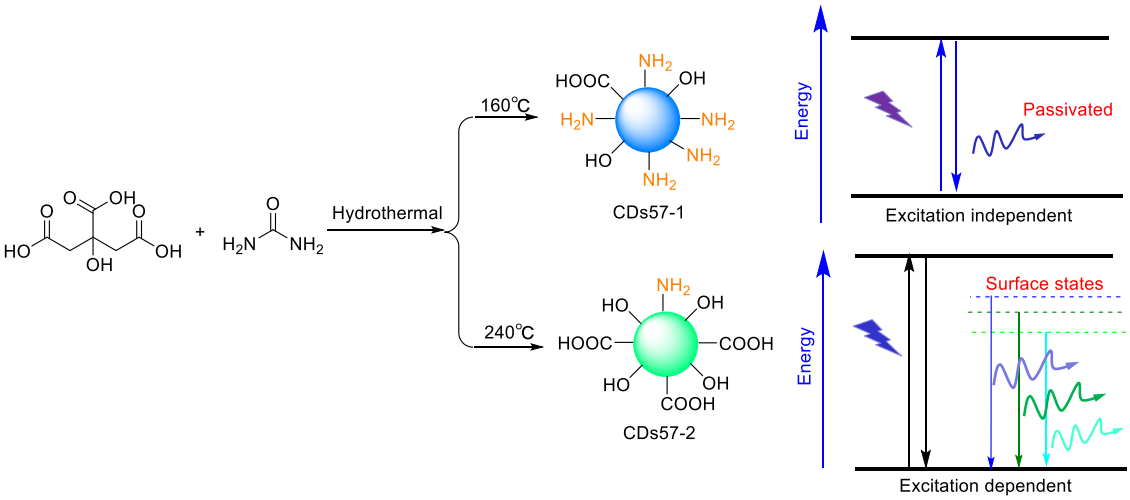

Fig. 57 Schematic presentation of CDs57 fabrication and its fluorescence mechanism

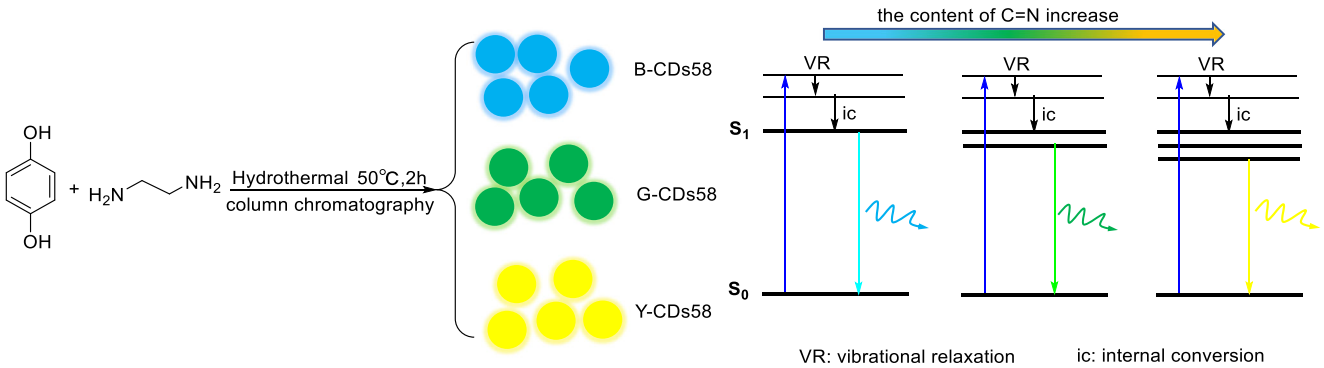

Fig. 58 Schematic presentation of CDs58 fabrication and its fluorescence mechanism

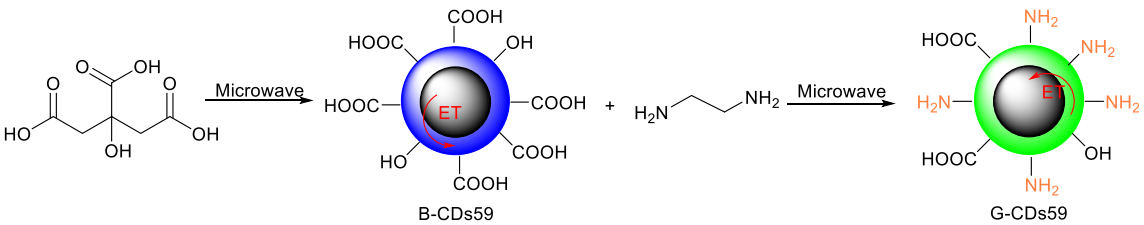

Fig. 59 Schematic presentation of CDs59 fabrication

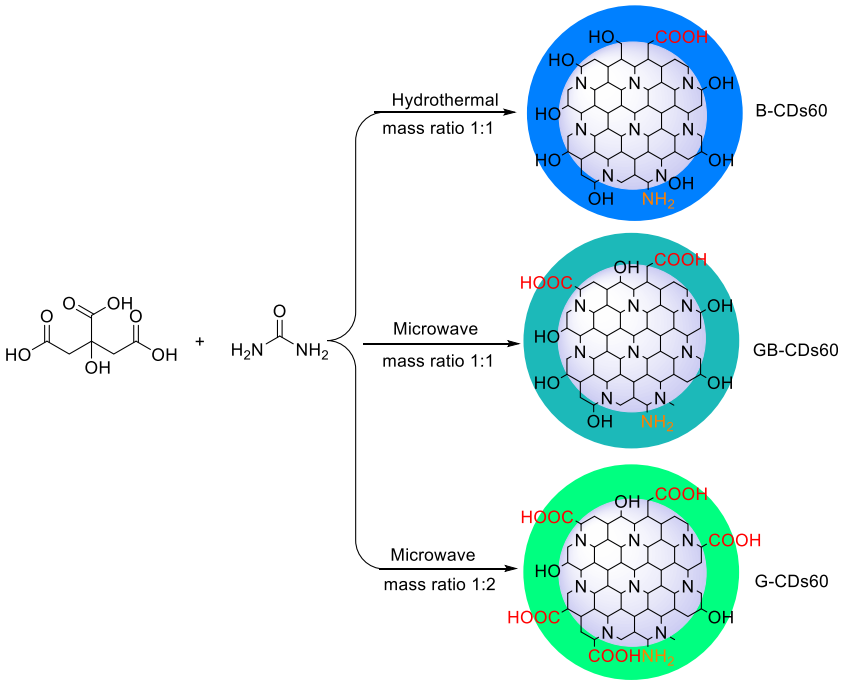

Fig. 60 Schematic presentation of CDs60 fabrication

QYs of B-CDs59 and G-CDs59 were 7.2 and 21.8%, respectively. The multicolor-emitting of CDs is mainly derived from carbon core and surface states. When -COOH is present on the surface of B-CDs59, electrons are transferred from carbon core to surface states. In contrast, when -NH_2 is present on the surface of G-CDs59, the orphaned electrons of nitrogen in

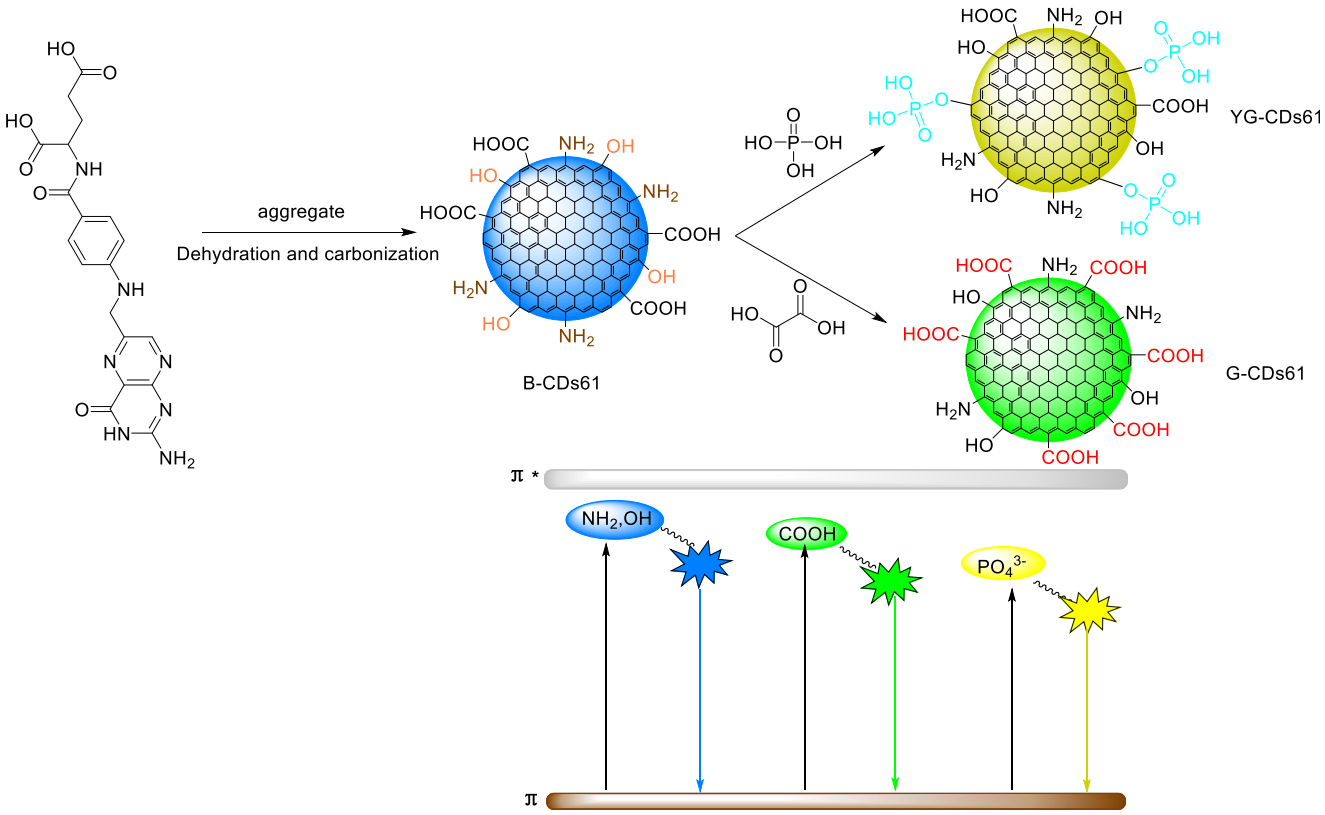

Fig. 61 Schematic presentation of CDs61 fabrication and its fluorescence mechanism

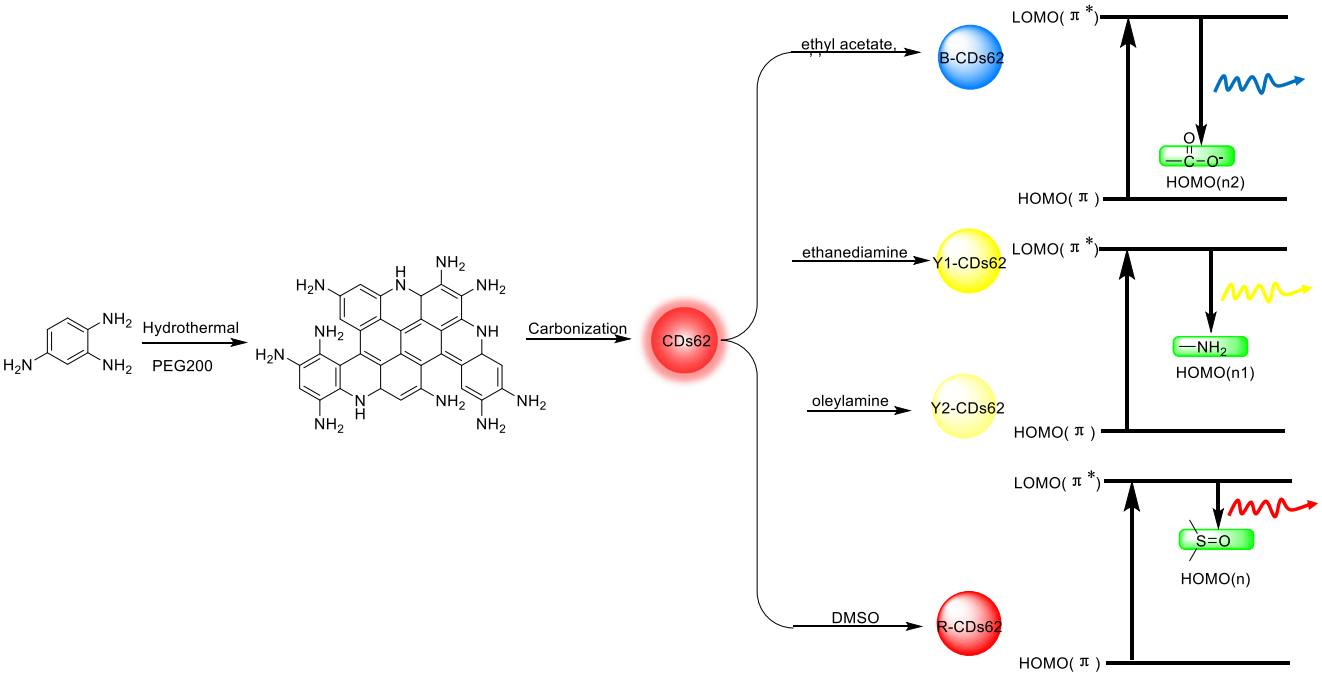

Fig. 62 Schematic presentation of CDs62 fabrication and its fluorescence mechanism

-NH_2 increases the electron density, reducing the energy gap of surface states, resulting in the red-shift of emission wavelength (Fig. 59).

Furthermore, controlling surface states using -COOH and -OH is a facile way to modulate the color-emitting of CDs. Sun et al. [133] synthesized bright blue-emitting CDs (B-CDs60) by hydrothermal method using CA and urea (mass ratio 1:1) as precursors. In the microwave method, the mass ratios were 1:1 and 1:2, and blue-green CDs (GB-CDs60) and green CDs (G-CDs60) were prepared. CDs60 exhibited excitation dependent, but the strongest emission redshift from 415 nm to 525 nm. Blue and green fluorescence are related to surface hydroxyl groups and carboxyl groups, respectively. Luminescent elastomers having strong tensile were prepared using CDs60. TiO2 nanowire arrays modified with CDs60 have potential applications in photovoltaic converters (Fig. 60).

Carboxyl groups and phosphate radical on CDs surface can introduce new energy levels into their electronic structures,

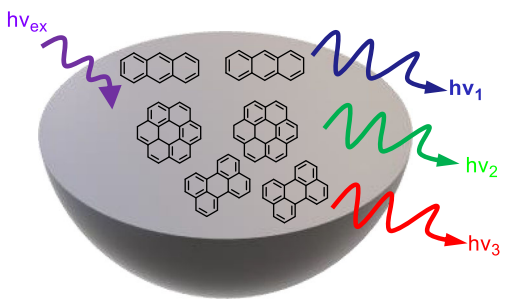

Fig. 63 The model system of CDs63 containing only three types of PAHs

resulting in CDs with tunable emission colors. B-CDs61 with a QY of about 31.59% were synthesized by using folic acid as the precursor [134]. Phosphoric acid and oxalic acid were used to modify the surface state of B-CDs61, resulting in the decrease of band gap energy and obtaining green and yellow-green CDs (G-CDs61 and YG-CDs61). The redshift of the treated CDs61 was 70 nm and 105 nm, respectively. The band gap energy before and after oxalic acid treatment was 2.35 eV and 1.75 eV, respectively. CDs61 as an efficient probe were applied in vitro and in vivo bioimaging (Fig. 61).

The function groups from different solvents can bring about different surface states and introduce new energy levels into their electronic structure, and thus contribute to the modulation of the color-emitting of CDs. Yuan et al. [135] fabricated long-wavelength red emission CDs62 using 1,2,4-triaminobenzen as carbon source and polyethylene glycol 200 (PEG200) as passivant through solvothermal method. Furthermore, multicolor-emitting CDs62 are observed when CDs62 are dissolved in ethyl acetate, ethanediamine, oleylamine and DMSO. Diverse function groups have different ability to donor electrons, S=O>-NH_2>-OCO-. Multicolor-emitting CDs62 can be used to construct warm WLEDs (Fig. 62).

The precursors with larger conjugate structures and high temperature conditions are more advantageous for obtaining long-wavelength emitting CDs. Fu et al. [136] designed a model system containing only three types of polycyclic aromatic hydrocarbons (PAHs) to mimic the optical properties of CDs63, in which anthracene, pyrene and perylene embedded in a matrix dominated by sp^3 hybrid carbon. The Stokes shift

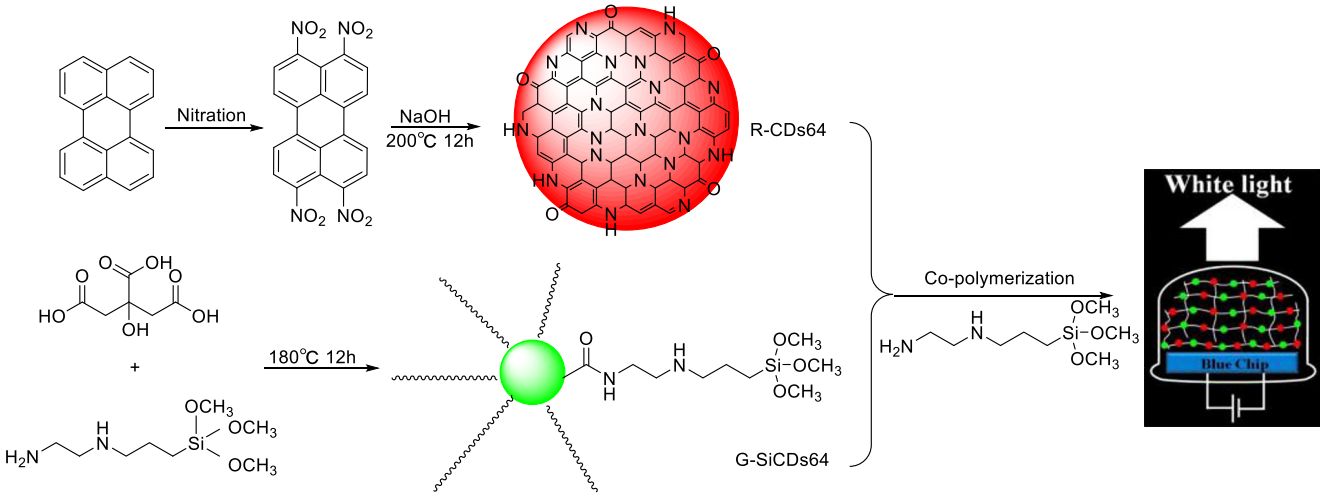

Fig. 64 Schematic presentation of R-CDs64 and G-SiCDs64 fabrication

is large due to exciton self-trapping in stacked PAHs molecules. The transfer of energy from PAHs with larger energy gaps to PAHs with smaller energy gaps, results in the red-shift of emission wavelength. CDs63 can be used for wavelength tunable nanolasers or organic light-emitting diodes (Fig. 63).

Increasing the quinone structure on the surface by alkali induced can tune the color-emitting of CDs. Yuan et al. [137] obtained alkali induced R-CDs64 using perylene with a large conjugated structure and strong fluorescence activity. In addition, green emission amino silane functionalized CDs (G-SiCDs64) were obtained by heating CA and N-(2-aminoethyl)-3-aminopropyltrimethoxysilane (AEATMS). The QYs of R-CDs64 and G-SiCDs64 were 80% and 49%, respectively. Since the alkali induced surface electronic states, the quinone structure of R-CDs64 increases, which is responsible for red emission. R-CDs64 were doped into the amino silane to achieve solid red light-emitting. G-SiCDs64/R-CDs64 gel glasses were prepared by doping R-CDs64 into G-SiCDs64 sol, which can be potentially applied in three-color WLEDs (Fig. 64).

Reasonable adjustment of surface oxidation degree or size can be beneficial to modulate the color-emitting of CDs. By carefully changing the nitric acid concentration and reaction conditions, the size and surface oxidation degree of CDs can be adjusted. The tunable color-emitting CDs65 were synthesized by oxidation and ultrafiltration of carbon fibers (CFs) [138]. The emission wavelengths of CDs65can be tuned from 430 to 610 nm. The higher the degree of surface oxidation or

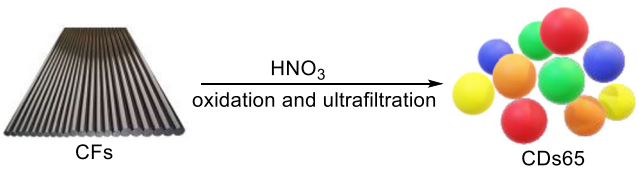

Fig. 65 Schematic presentation of CDs65 fabrication

conjugated system, the smaller the surface energy gap, resulting in the red-shift of emission wavelength. CDs65 as an efficient probe was applied in Vero cells imaging (Fig. 65).

Reasonable adjustment of surface functional groups or size also facilitates the modulation of the color-emitting of CDs. B-CDs66 with controllable size and surface functional groups were fabricated by using lauric gallate via heat treatment [139]. Moreover, the ester groups on the surface of B-CDs66 can be turned into carboxylate groups by basic hydrolysis to gain G-CDs66. Nucleation-related emission dominated the fluorescence characteristics of B-CDs66, while the carboxyl as the surface emission traps induced the red shift emission of the de-esterified G-CDs66 (Fig. 66).

By varying the composition of four different solvents during the synthesis, the size and graphite N content of CDs can be changed, and the color-emitting of CDs was finally modulated. Ding et al. [140] synthesized CDs67 using L-glutamic acid and o-phenylenediamine via solvothermal method. By changing four different solvents in synthetic process, CDs exhibited tunable emission colors from blue (443 nm) to NIR (745 nm). The QYs of B -, G -, Y -, and R -CDs67 are 54%, 41%, 51%, and 43%, respectively. CDs67 had large conjugated π-domains and rich surface functional groups. CDs67 have been successfully used to make CDs67/PVA films and as bioimaging fluorescent probes (Fig. 67).

By changing the composition of reaction solvents, the size and bandgaps of CDs were systematically manipulated, thereby modulating the color-emitting of CDs from blue to red. Based on the molecular fusion mechanism, Zhan et al. [141] fabricated multicolor-emitting CDs68 by changing the composition of reaction solvents using 1,3,6- trinitropyrene (TNP) as the carbon and nitrogen sources. The QY of CDs68 was up to 59%. The color-emitting of CDs68 whose surface were passivated by nitrogen-containing groups can be modulated by QCE and slightly altered by surface functional groups.

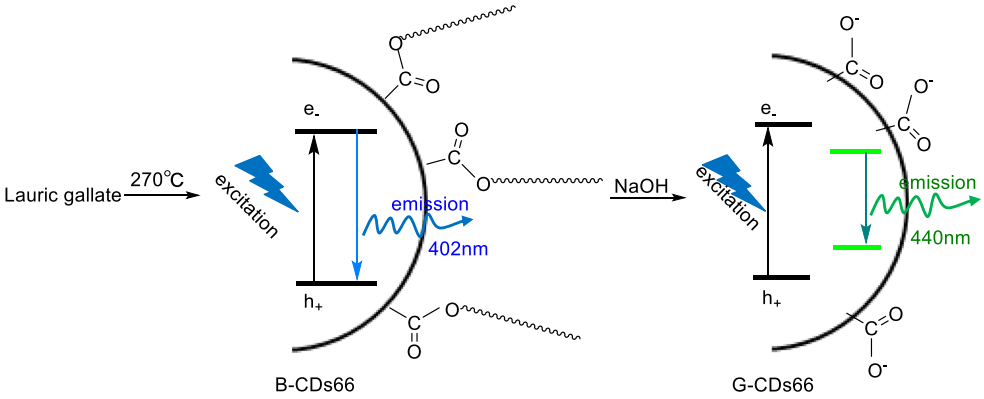

Fig. 66 Schematic presentation of B-CDs66 and G-CDs66 fabrication and its fluorescence mechanism

Fluorescence imaging study in Hela cells and the Hela tumor-bearing nude mice served to assess the bioimaging capabilities of lipo-R-CDs68 in vitro and in vivo (Fig. 68).

The color-emitting of CDs can be modulated by varying the concentration. Chen et al. [142] fabricated the concentration dependent CDs69 using CA and ethanolamine by hydrothermal method. The color tunable fluorescent CDs69 with emission wavelengths ranging from 585 to 514 nm. Surface, edge, and core states were three fluorescent centers in CDs69. The pyrrolic-N at the surface of CDs69 was the fluorescent center of orange light. Under the action of dimethylformamide solvent, CDs69 showed stronger emission than that in water. In addition, there was an energy transfer process between three fluorescent centers. Concentration-induced CDs69 have been used to prepare warm white LED (Fig. 69).

Surface states mechanism is considered to be the key fluorescence mechanism of CDs, which provides a primary way to modulate the color-emitting of CDs. Controlling the surface

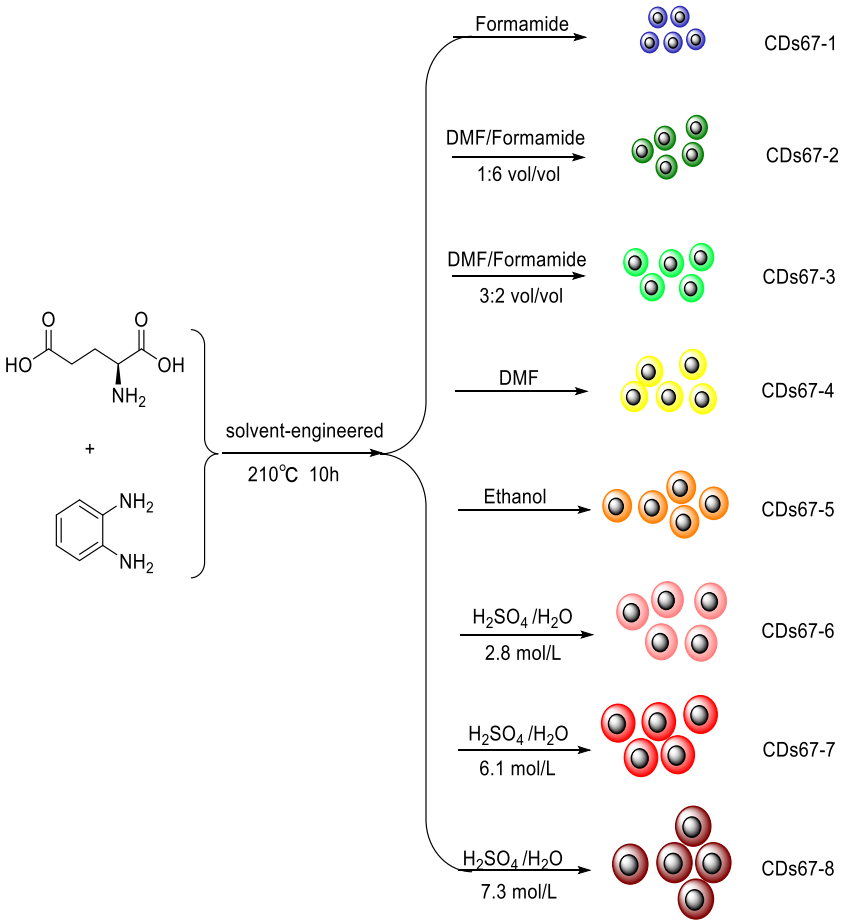

Fig. 67 Schematic presentation of CDs67 fabrication

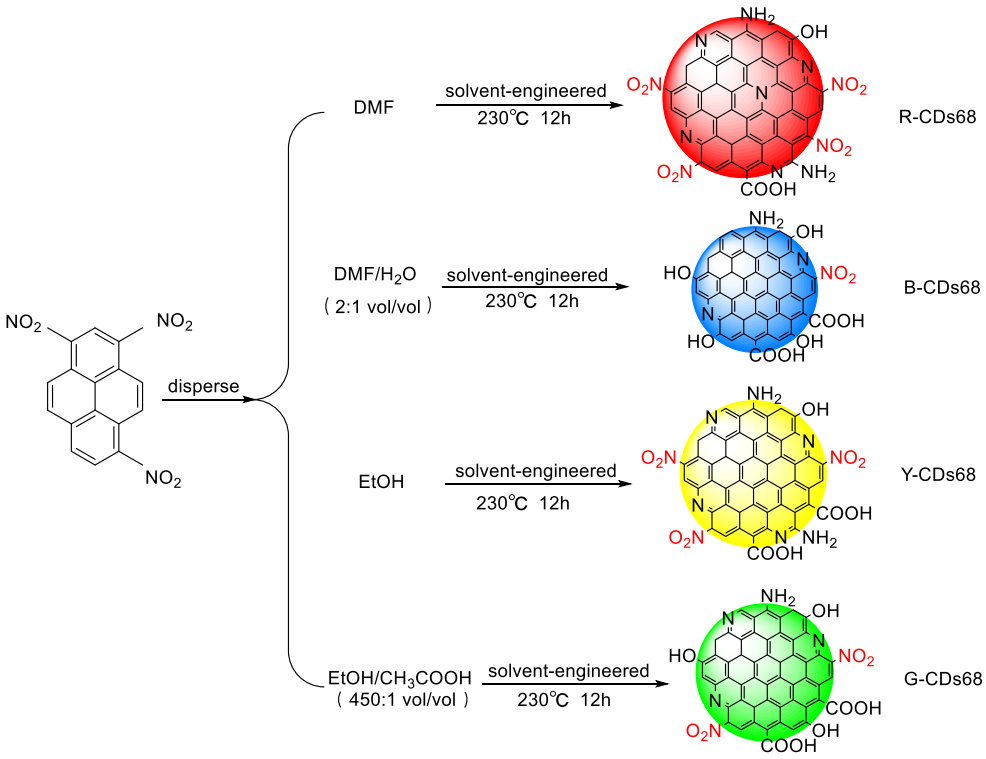

Fig. 68 Schematic presentation of CDs68 fabrication

states and element doping are facile and effective way to improve the optical properties of CDs. In particular, N-related functional groups produced by doping will have a great effect on the color-emitting of CDs.

It is unclear how different preparation methods or precursors affect the fluorescence mechanism of CDs. The use of natural starting materials (such as leafs, bark, coffee beans, menure, etc.) that are available in certain regions only makes method hardly reproducible by others. Users prefer methods that are based on the use of materials that are available (a) anywhere, (b) at any time (not just during certain seasons), and (c) in constant quality. If CDs are prepared with pure organic chemicals, different effects may occur. Defined organic chemicals such as CA is the most commonly used precursor at the moment, because the reproducible preparation of CDs is particularly sensitive to the kind of starting material. However, under the same synthesis conditions, precursors with larger conjugate structures and intense fluorescence activities are more advantageous for obtaining long-wavelength emissions CDs. These precursors facilitate the self-assembly of carbon core, and the different functional groups in precursors will contribute to the formation of the surface state of CDs.

Furthermore, the solvents can adjust the dehydration and carbonization of precursors. By simply varying the composition of reaction solvents, the bandgaps of CDs also can be manipulated, modulating the color-emitting of CDs (Table 5).

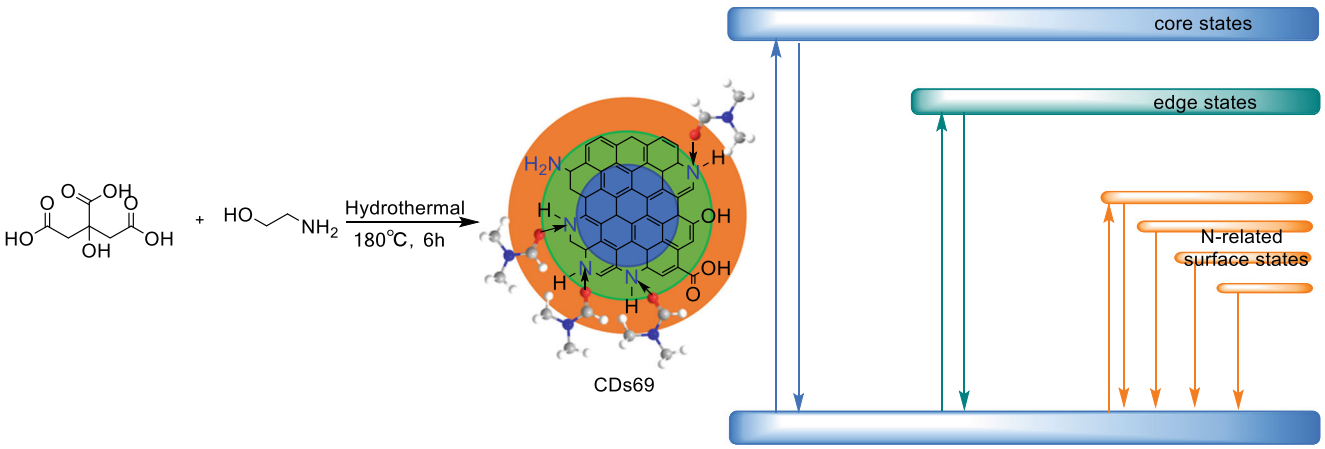

Fig. 69 Schematic presentation of CDs69 fabrication and its fluorescence mechanism

Table 5 An overview on multicolor-emitting carbon dots

Types	Particle composition	Particle Size(nm)	Ex/Em (nm)	QY (%)	Lifetime	Ref
B-CDs1	C, H, O, N	1.7	375/448	32	–	[30]
G-CDs1	C, H, O, N	2.8	375/550	13	–	
R-CDs1	C, H, O, N	4.5	375/638	8	–	
B-CDs2	C, H, O, N	1.95	365/430	75	14.2	[31]
G-CDs2	C, H, O, N	2.41	365/513	73	12.2	
Y-CDs2	C, H, O, N	3.78	365/535	58	11.3	
O-CDs2	C, H, O, N	4.90	365/565	53	8.8	
R-CDs2	C, H, O, N	6.68	365/604	12	6.8	
B-CDs3	C, H, O, N	3.96 ± 0.54	360/440	52.6	–	[23]
G-CDs3	C, H, O, N	4.12 ± 0.68	470/550	35.1	–	
R-CDs3	C, H, O, N	4.34 ± 0.49	550/600	12.9	–	
B-CDs4	C, H, O, N	2.6	370/440	35	–	[42]
G-CDs4	C, H, O, N	2.6	390/553	–	–	
Y-CDs4	C, H, O, N	2.6	470/580	–	–	
R-CDs4	C, H, O, N	2.6	510/625	24	–	
G-CDs5	C, H, O, N	6.53	460/515	81	5.74	[43]
R-CDs5	C, H, O, N	6.45	560/610	80	8.26	
B-CDs9	C, H, O, N	6	365/435	4.8	0.99	[63]
G-CDs9	C, H, O, N	8.2	365/535	17.6	4.44	
R-CDs9	C, H, O, N	10	365/604	26.1	9.39	
B-CDs10	C, H, O, N	6.8	390/466	11.9	3.2	[64]
Y-CDs10	C, H, O, N	6.8	450/555	16.7	0.87	
R-CDs10	C, H, O, N	6.8	540/637	26.2	0.68	
CDs11–1	C, H, O, N	3–6	370/442	3.4	6	[65]
CDs11–2	C, H, O, N	3–6	370/458	6.3	6	
CDs11–3	C, H, O, N	3–6	370/458	11.7	6.3	
CDs11–4	C, H, O, N	3–6	370/443	13.6	6.6	
CDs11–5	C, H, O, N	3–6	370/458	53.7	7.9	
CDs11–6	C, H, O, N	3–6	370/460	60.5	7.5	
B-CDs12	C, H, O, N	2–3	365/460	13.3	–	[69]
G-CDs12	C, H, O, N	2–3	365/510	10	–	
Y-CDs12	C, H, O, N	2–3	365/550	11.6	–	
R-CDs12	C, H, O, N	2–3	365/630	4	–	
B-CDs13	C, H, O, N	4.2	360/444	14.3	2.7–3.1	[70]
Y-CDs13	C, H, O, N	3.8	450/533	45	2.7–3.1	
O-CDs13	C, H, O, N	3.7	530/574	7.5	2.7–3.1	
CDs15–1	C, H, O, N, S	3.9	400/482	–	–	[74]
CDs15–2	C, H, O, N, S	4.3	400/524	–	–	
CDs15–3	C, H, O, N, S	3.5	400/570	–	–	
CDs15–4	C, H, O, N, S	3.1	400/609	–	–	
CDs15–5	C, H, O, N, S	4.1	400/628	–	–	
CDs15–6	C, H, O, N, S	3.8	400/680			
B-CDs17	C, H, O, N, B	2 ± 1	360/452	39	11.9	[78]
N-CDs17	C, H, O, N	2 ± 1	360/452	64	12.8	
P-CDs17	C, H, O, N, P	2 ± 1	360/452	70	13	
F-CDs18	C, H, O, N, F	5.52	480/540	31	–	[79]
CDs18	C, H, O, N	5.18	400/490	28	–	
CDs20	C, H, O, N	2.68	450/550	46	8.11	[85]
Mn-CDs20	C, H, O, N, Mn	2.95	450/555	68.6	8.75	
CDs22	C, H, O, N	–	365/450	12	5.5	[87]
Zn-CDs22	C, H, O, N, Zn	2–5	450/575	51.2	6.8	
G-CDs55	C, H, O, N	20 ± 8	410/518	35.3	4.49	[129]

Table 5 (continued)

Types	Particle composition	Particle Size(nm)	Ex/Em (nm)	QY (%)	Lifetime	Ref
Y-CDs55	C, H, O, N	20 ± 8	400/543	17.5	3.84	
B-CDs56	C, H, O, N	1–12	360/480	–	–	[130]
Y-CDs56	C, H, O, N	2–8	460/600	–	–	
R-CDs56	C, H, O, N	5–11	635/710	–	–	
CDs57	C, H, O, N	5	360/440	44.7	7.13	[131]
CDs57	C, H, O, N	–	320/410	20.8	5.21	
B-CDs58	C, H, O, N	100	380/465	9.32	2.89	[127]
G-CDs58	C, H, O, N	100	410/510	78.68	4.01	
Y-CDs58	C, H, O, N	100	355/550	1.47	0.89	
B-CDs59	C, H, O, N	3.5 ± 0.3	340/440	7.2	–	[132]
G-CDs59	C, H, O, N	3.5 ± 0.3	340/440	21.8	–	
B-CDs60	C, H, O, N	2–9	320/415	–	5.21	[133]
GB-CDs60	C, H, O, N	1–5	360/460	–	9.85	
G-CDs60	C, H, O, N	1–5	400/525	–	5.84	
B-CDs61	C, H, O, N	2–5	380/445	31.59	–	[134]
YG-CDs61	C, H, O, N, P	–	400/550	–	–	
G-CDs61	C, H, O, N	–	385/515	–	–	
CDs62	C, H, O, N	4.5	420/625	15	3.59	[135]
B-CDs62	C, H, O	4.5	373/473 460/621	25	7.68	
Y1-CDs62	C, H, O, N	4.5	460/560	18.3	4.23	
Y2-CDs62	C, H, O, N	4.5	460/560	15.9	4.02	
R-CDs62	C, H, O, N	4.5	464/624	10.8	3.16	
R-CDs64	C, H, O, N	5–8	560/610	80	–	[137]
G-SiCDs64	C, H, O, N, Si	6	460/511	49	–	
CDs65	C, H, O, N	2.7–4.1	360/430–610	–	–	[138]
B-CDs66	C, H, O	2	330/402	–	2.32	[139]
G-CDs66	C, H, O	2	330/440	–	3.95	
CDs67–1	C, H, O, N	1.8	389/443	54.2	10.18	[140]
CDs67–2	C, H, O, N	3.1	458/515	40.9	8.43	
CDs67–3	C, H, O, N	–	489/544	34.8	–	
CDs67–4	C, H, O, N	5.2	512/571	51.3	4.47	
CDs67–5	C, H, O, N	–	535/594	47.9	–	
CDs67–6	C, H, O, N	–	563/640	48.7	–	
CDs67–7	C, H, O, N	7.6	634/715	43.2	2.14	
CDs67–8	C, H, O, N	–	661/745	12.8	–	
B-CDs68	C, H, O, N	2.25	380/460	6.4	4.9	[141]
G-CDs68	C, H, O, N	2.49	460/517	7.1	6	
Y-CDs68	C, H, O, N	2.93	510/581	59	6.33	
R-CDs68	C, H, O, N	3.98	550/620	27.4	6.42	
CDs69–1	C, H, O, N	3.7	375/617	–	9.29	[142]
CDs69–2	C, H, O, N	3.7	375/607	–	12.4	
CDs69–3	C, H, O, N	3.7	375/570	–	16.31	
CDs69–4	C, H, O, N	3.7	375/490	–	13.57	
CDs69–5	C, H, O, N	3.7	375/477	–	5.89	
CDs69–6	C, H, O, N	3.7	375/470	–	7.19	
CDs69–7	C, H, O, N	3.7	375/460	–	4.87	
CDs69–8	C, H, O, N	3.7	375/450	–	5.95	
CDs69–9	C, H, O, N	3.7	375/430	–	4.87	
CDs69–9	C, H, O, N	3.7	375/430	–	4.49	

Conclusion

In this review, we summarized the fluorescence mechanism of CDs and focused on the modulation of different color-emitting CDs. The fluorescence of CDs is usually believed to originate from the carbon-core states and surface states. Among them, surface states mechanism was considered to be the key fluorescence mechanism of CDs. Controlling the surface states is the most primary and easy method to modulate the color-emitting of CDs. Different functional groups can form various surface defect states, thus introducing many energy level band gaps to regulate the color-emitting of CDs. In addition, element doping (with nitrogen, sulfur, other heteroatoms and metal ions) is a facile and effective way to improve the optical properties of CDs. In particular, N-related functional groups produced by doping will have a great effect on the color-emitting of CDs. For some CDs with large conjugated π-domains and few surface chemical groups, the bandgap of conjugated π-domains is considered to be the carbon-core states fluorescence center. However, it is difficult to control the size of the conjugated π-domains in CDs, so the quantum size effect is not easy to use modulate the color-emitting of CDs. Some fluorescent small molecules or fluorophores are attached to the surface or interior of carbon skeleton and can show fluorescence emission directly. There are few literatures on the use of molecule states mechanisms to modulate the color-emitting of CDs, because reactions are difficult to be controlled. Once the chemical structure of CDs is well controlled during the synthesis process, it is possible to clarify the fluorescence mechanism of CDs and large-scale synthesis different color-emitting CDs, and eventually promote the use of CDs in biomedicine and optoelectronics fields in future work.

Acknowledgements The work was supported by the National Natural Science Foundation of China (51678409, 51638011 and 51578375), Tianjin Research Program of Application Foundation and Advanced Technology (18JCYBJC87500, 15ZCZDSF00880), State Key Laboratory of Separation Membranes and Membrane Processes (Z1-201507), and the Program for Innovative Research Team in University of Tianjin (TD13-5042).

Compliance with ethical standards The author(s) declare that they have no competing interests.

References

1. Ding C, Zhu A, Tian Y (2014) Functional surface engineering of C-dots for fluorescent biosensing and in vivo bioimaging. Acc Chem Res 47(1):20–30
2. Fernando KAS, Sahu S, Liu Y, Lewis WK, Guliants EA, Jafariyan A, Wang P, Bunker CE, Sun Y-P (2015) Carbon quantum dots and applications in photocatalytic energy conversion. ACS Appl Mater Interfaces 7(16):8363–8376
3. Yang P, Zhao J, Zhang L, Li L, Zhu Z (2015) Intramolecular hydrogen bonds quench photoluminescence and enhance photocatalytic activity of carbon Nanodots. Chem Eur J 21(23): 8561–8568
4. Hao T, Wei X, Nie Y, Xu Y, Yan Y, Zhou Z (2016) An eco-friendly molecularly imprinted fluorescence composite material based on carbon dots for fluorescent detection of 4-nitrophenol. Microchim Acta 183(7):2197–2203
5. Simões EFC, Leitão JMM, da Silva JCGE (2016) Carbon dots prepared from citric acid and urea as fluorescent probes for hypochlorite and peroxynitrite. Microchim Acta 183(5):1769–1777
6. Yao W, Wu N, Lin Z, Chen J, Li S, Weng S, Zhang L, Liu A, Lin X (2017) Fluorescent turn-off competitive immunoassay for biotin based on hydrothermally synthesized carbon dots. Microchim Acta 184(3):907–914
7. Li X, Liu Y, Song X, Wang H, Gu H, Zeng H (2015) Intercrossed carbon Nanorings with pure surface states as low-cost and environment-friendly phosphors for white-light-emitting diodes. Angew Chem Int Ed 54(6):1759–1764
8. Zhu Z, Ma J, Wang Z, Mu C, Fan Z, Du L, Bai Y, Fan L, Yan H, Phillips DL, Yang S (2014) Efficiency enhancement of perovskite solar cells through fast Electron extraction: the role of graphene quantum dots. J Am Chem Soc 136(10):3760–3763
9. Liu J, Liu C, Zhou Z (2019) A turn-on fluorescent sulfide probe prepared from carbon dots and MnO2 nanosheets. Microchim Acta 186(5):281
10. Wang Y, Yang Y, Liu W, Ding F, Zou P, Wang X, Zhao Q, Rao H (2019) A carbon dot-based ratiometric fluorometric and colorimetric method for determination of ascorbic acid and of the activity of ascorbic acid oxidase. Microchim Acta 186(4):246
11. Ning Y, Hu J, Wei K, He G, Wu T, Lu F (2019) Fluorometric determination of mercury(II) via a graphene oxide-based assay using exonuclease III-assisted signal amplification and thymidine-Hg(II)-thymidine interaction. Microchim Acta 186(4):216
12. Zhao A, Chen Z, Zhao C, Gao N, Ren J, Qu X (2015) Recent advances in bioapplications of C-dots. Carbon 85:309–327
13. Zuo P, Lu X, Sun Z, Guo Y, He H (2016) A review on syntheses, properties, characterization and bioanalytical applications of fluorescent carbon dots. Microchim Acta 183(2):519–542
14. Miao Q, Li S, Han S, Wang Z, Wu Y, Nie G (2012) Construction of hydroxypropyl-β-cyclodextrin copolymer nanoparticles and targeting delivery of paclitaxel. J Nanopart Res 14(8):1043
15. Ge J, Lan M, Zhou B, Liu W, Guo L, Wang H, Jia Q, Niu G, Huang X, Zhou H, Meng X, Wang P, Lee C-S, Zhang W, Han X (2014) A graphene quantum dot photodynamic therapy agent with high singlet oxygen generation. Nat Commun 5:4596
16. Pirsaheb M, Mohammadi S, Salimi A, Payandeh M (2019) Functionalized fluorescent carbon nanostructures for targeted imaging of cancer cells: a review. Microchim Acta 186(4):231
17. Wang C, Jiang K, Wu Q, Wu J, Zhang C (2016) Green synthesis of red-emitting carbon Nanodots as a novel "turn-on" Nanothermometer in living cells. Chemistry 22(41):14475–14479
18. Roy P, Chen P-C, Periasamy AP, Chen Y-N, Chang H-T (2015) Photoluminescent carbon nanodots: synthesis, physicochemical properties and analytical applications. Mater Today 18(8):447–458
19. Zhu S, Tang S, Zhang J, Yang B (2012) Control the size and surface chemistry of graphene for the rising fluorescent materials. Chem Commun 48(38):4527–4539
20. Yeh T-F, Teng C-Y, Chen S-J, Teng H (2014) Nitrogen-doped graphene oxide quantum dots as Photocatalysts for overall water-splitting under visible light illumination. Adv Mater 26(20):3297–3303
21. Zhu S, Song Y, Zhao X, Shao J, Zhang J, Yang B (2015) The photoluminescence mechanism in carbon dots (graphene quantum dots, carbon nanodots, and polymer dots): current state and future perspective. Nano Res 8(2):355–381

22. Yan F, Jiang Y, Sun X, Bai Z, Zhang Y, Zhou X (2018) Surface modification and chemical functionalization of carbon dots: a review. Microchim Acta 185(9):424
23. Miao X, Qu D, Yang D, Nie B, Zhao Y, Fan H, Sun Z (2018) Synthesis of carbon dots with multiple color emission by controlled graphitization and surface functionalization. Adv Mater 30(1):1704740
24. Sk MA, Ananthanarayanan A, Huang L, Lim KH, Chen P (2014) Revealing the tunable photoluminescence properties of graphene quantum dots. J Mater Chem C 2(34):6954–6960
25. Kwon W, Lee G, Do S, Joo T, Rhee S-W (2014) Size-controlled soft-template synthesis of carbon Nanodots toward versatile photoactive materials. Small 10(3):506–513
26. Zhang T, Zhu GY, Yu CH, Xie Y, Xia MY, Lu BY, Fei X, Peng Q (2019) The UV absorption of graphene oxide is size-dependent: possible calibration pitfalls. Microchim Acta 186(3):207
27. Krishnamoorthy K, Veerapandian M, Mohan R, Kim S-J (2012) Investigation of Raman and photoluminescence studies of reduced graphene oxide sheets. Applied Physics A 106(3):501–506
28. Bhattacharya A, Chatterjee S, Prajapati R, Mukherjee TK (2015) Size-dependent penetration of carbon dots inside the ferritin nanocages: evidence for the quantum confinement effect in carbon dots. Phys Chem Chem Phys 17(19):12833–12840
29. Liang Q, Ma W, Shi Y, Li Z, Yang X (2013) Easy synthesis of highly fluorescent carbon quantum dots from gelatin and their luminescent properties and applications. Carbon 60:421–428
30. Tian Z, Zhang X, Li D, Zhou D, Jing P, Shen D, Qu S, Zboril R, Rogach AL (2017) Full-color inorganic carbon dot phosphors for white-light-emitting diodes. Adv Opt Mater 5(19):1700416
31. Yuan F, Wang Z, Li X, Li Y, Tan Z, Fan L, Yang S (2017) Bright multicolor bandgap fluorescent carbon quantum dots for electroluminescent light-emitting diodes. Adv Mater 29(3):1604436
32. Shen J, Zhu Y, Yang X, Zong J, Zhang J, Li C (2012) One-pot hydrothermal synthesis of graphene quantum dots surface-passivated by polyethylene glycol and their photoelectric conversion under near-infrared light. New J Chem 36(1):97–101
33. Shen J, Zhu Y, Yang X, Li C (2012) Graphene quantum dots: emergent nanolights for bioimaging, sensors, catalysis and photovoltaic devices. Chem Commun 48(31):3686–3699
34. Du J, Wang H, Wang L, Zhu S, Song Y, Yang B, Sun H (2016) Insight into the effect of functional groups on visible-fluorescence emissions of graphene quantum dots. J Mater Chem C 4(11): 2235–2242
35. Zhang X, Zhang Y, Wang Y, Kalytchuk S, Kershaw SV, Wang Y, Wang P, Zhang T, Zhao Y, Zhang H, Cui T, Wang Y, Zhao J, Yu WW, Rogach AL (2013) Color-switchable electroluminescence of carbon dot light-emitting diodes. ACS Nano 7(12):11234–11241
36. Sachdev A, Matai I, Gopinath P (2014) Implications of surface passivation on physicochemical and bioimaging properties of carbon dots. RSC Adv 4(40):20915–20921
37. Jiang K, Wang Y, Cai C, Lin H (2018) Conversion of carbon dots from fluorescence to Ultralong room-temperature phosphorescence by heating for security applications. Adv Mater 30(26): e1800783
38. Zhang Y, Hu Y, Lin J, Fan Y, Li Y, Lv Y, Liu X (2016) Excitation wavelength Independence: toward low-threshold amplified spontaneous emission from carbon Nanodots. ACS Appl Mater Interfaces 8(38):25454–25460
39. Kiran S, Misra RDK (2015) Mechanism of intracellular detection of glucose through nonenzymatic and boronic acid functionalized carbon dots. J Biomed Mater Res A 103(9):2888–2897
40. Yang H, Li F, Zou C, Huang Q, Chen D (2017) Sulfur-doped carbon quantum dots and derived 3D carbon nanoflowers are effective visible to near infrared fluorescent probes for hydrogen peroxide. Microchim Acta 184(7):2055–2062
41. Xu Y, Wu M, Feng X-Z, Yin X-B, He X-W, Zhang Y-K (2013) Reduced carbon dots versus oxidized carbon dots: photo- and Electrochemiluminescence investigations for selected applications. Chem Eur J 19(20):6282–6288
42. Ding H, Yu SB, Wei JS, Xiong HM (2016) Full-color light-emitting carbon dots with a surface-state-controlled luminescence mechanism. ACS Nano 10(1):484–491
43. Yuan B, Guan S, Sun X, Li X, Zeng H, Xie Z, Chen P, Zhou S (2018) Highly efficient carbon dots with reversibly switchable green-red emissions for trichromatic white light-emitting diodes. ACS Appl Mater Interfaces 10(18):16005–16014
44. Shen Z, Zhang C, Yu X, Li J, Wang Z, Zhang Z, Liu B (2018) Microwave-assisted synthesis of cyclen functional carbon dots to construct a ratiometric fluorescent probe for tetracycline detection. J Mater Chem C 6(36):9636–9641
45. Pan D, Zhang J, Li Z, Wu M (2010) Hydrothermal route for cutting graphene sheets into blue-luminescent graphene quantum dots. Adv Mater 22(6):734–738
46. Gude V, Das A, Chatterjee T, Mandal PK (2016) Molecular origin of photoluminescence of carbon dots: aggregation-induced orange-red emission. Phys Chem Chem Phys 18(40):28274–28280
47. Hu C, Su T-R, Lin T-J, Chang C-W, Tung K-L (2018) Yellowish and blue luminescent graphene oxide quantum dots prepared via a microwave-assisted hydrothermal route using H2O2 and KMnO4 as oxidizing agents. New J Chem 42(6):3999–4007
48. Song Y, Zhu S, Zhang S, Fu Y, Wang L, Zhao X, Yang B (2015) Investigation from chemical structure to photoluminescent mechanism: a type of carbon dots from the pyrolysis of citric acid and an amine. J Mater Chem C 3(23):5976–5984
49. Ehrat F, Bhattacharyya S, Schneider J, Lof A, Wyrwich R, Rogach AL, Stolarczyk JK, Urban AS, Feldmann J (2017) Tracking the source of carbon dot photoluminescence: aromatic domains versus molecular fluorophores. Nano Lett 17(12):7710–7716
50. D'Angelis d ESBC, Corrêa JR, Medeiros GA, Barreto G, Magalhães KG, de Oliveira AL, Spencer J, Rodrigues MO, BAD N (2015) Carbon dots (C-dots) from cow manure with impressive subcellular selectivity tuned by simple chemical modification. Chem Eur J 21(13):5055–5060
51. Teng X, Ma C, Ge C, Yan M, Yang J, Zhang Y, Morais PC, Bi H (2014) Green synthesis of nitrogen-doped carbon dots from konjac flour with "off–on" fluorescence by Fe3+ and l-lysine for bioimaging. J Mater Chem B 2(29):4631–4639
52. Wang L, Cao HX, Pan CG, He YS, Liu HF, Zhou LH, Li CQ, Liang GX (2018) A fluorometric aptasensor for bisphenol a based on the inner filter effect of gold nanoparticles on the fluorescence of nitrogen-doped carbon dots. Microchim Acta 186(1):28
53. Liu Y, Tang X, Deng M, Cao Y, Li Y, Zheng H, Li F, Yan F, Lan T, Shi L, Gao L, Huang L, Zhu T, Lin H, Bai Y, Qu D, Huang X, Qiu F (2019) Nitrogen doped graphene quantum dots as a fluorescent probe for mercury(II) ions. Microchim Acta 186(3):140
54. Wu WC, Chen HT, Lin SC, Chen HY, Chen FR, Chang HT, Tseng FG (2019) Nitrogen-doped carbon nanodots prepared from polyethylenimine for fluorometric determination of salivary uric acid. Microchim Acta 186(3):166
55. Niino S, Takeshita S, Iso Y, Isobe T (2016) Influence of chemical states of doped nitrogen on photoluminescence intensity of hydrothermally synthesized carbon dots. J Lumin 180:123–131
56. Yuan K, Zhang X, Qin R, Ji X, Cheng Y, Li L, Yang X, Lu Z, Liu H (2018) Surface state modulation of red emitting carbon dots for white light-emitting diodes. J Mater Chem C 6(46):12631–12637
57. Mintz KJ, Zhou Y, Leblanc RM (2019) Recent development of carbon quantum dots regarding their optical properties, photoluminescence mechanism, and core structure. Nanoscale 11(11):4634–4652
58. Wang Y, Zhuang Q, Ni Y (2015) Facile microwave-assisted solid-phase synthesis of highly fluorescent nitrogen–sulfur-Codoped

carbon quantum dots for cellular imaging applications. Chem Eur J 21(37):13004–13011
59. Zhang H, Chen Y, Liang M, Xu L, Qi S, Chen H, Chen X (2014) Solid-phase synthesis of highly fluorescent nitrogen-doped carbon dots for sensitive and selective probing ferric ions in living cells. Anal Chem 86(19):9846–9852
60. Zhou X, Zhao G, Tan X, Qian X, Zhang T, Gui J, Yang L, Xie X (2019) Nitrogen-doped carbon dots with high quantum yield for colorimetric and fluorometric detection of ferric ions and in a fluorescent ink. Microchim Acta 186(2):67
61. Saberi Z, Rezaei B, Ensafi AA (2019) Fluorometric label-free aptasensor for detection of the pesticide acetamiprid by using cationic carbon dots prepared with cetrimonium bromide. Microchim Acta 186(5):273
62. Lu KH, Lin JH, Lin CY, Chen CF, Yeh YC (2019) A fluorometric paper test for chromium(VI) based on the use of N-doped carbon dots. Microchim Acta 186(4):227
63. Jiang K, Sun S, Zhang L, Lu Y, Wu A, Cai C, Lin H (2015) Red, green, and blue luminescence by carbon dots: full-color emission tuning and multicolor cellular imaging. Angew Chem Int Ed Eng 54(18):5360–5363
64. Pan L, Sun S, Zhang A, Jiang K, Zhang L, Dong C, Huang Q, Wu A, Lin H (2015) Truly fluorescent excitation-dependent carbon dots and their applications in multicolor cellular imaging and multidimensional sensing. Adv Mater 27(47):7782–7787
65. Yuan YH, Liu ZX, Li RS, Zou HY, Lin M, Liu H, Huang CZ (2016) Synthesis of nitrogen-doping carbon dots with different photoluminescence properties by controlling the surface states. Nanoscale 8(12):6770–6776
66. Hu C, Liu Y, Yang Y, Cui J, Huang Z, Wang Y, Yang L, Wang H, Xiao Y, Rong J (2013) One-step preparation of nitrogen-doped graphene quantum dots from oxidized debris of graphene oxide. J Mater Chem B 1(1):39–42
67. Liu J, Liu X, Luo H, Gao Y (2014) One-step preparation of nitrogen-doped and surface-passivated carbon quantum dots with high quantum yield and excellent optical properties. RSC Adv 4(15):7648–7654
68. Lan M, Di Y, Zhu X, Ng T-W, Xia J, Liu W, Meng X, Wang P, Lee C-S, Zhang W (2015) A carbon dot-based fluorescence turn-on sensor for hydrogen peroxide with a photo-induced electron transfer mechanism. Chem Commun 51(85):15574–15577
69. Hola K, Sudolska M, Kalytchuk S, Nachtigallova D, Rogach AL, Otyepka M, Zboril R (2017) Graphitic nitrogen triggers red fluorescence in carbon dots. ACS Nano 11(12):12402–12410
70. Liu C, Wang R, Wang B, Deng Z, Jin Y, Kang Y, Chen J (2018) Orange, yellow and blue luminescent carbon dots controlled by surface state for multicolor cellular imaging, light emission and illumination. Microchim Acta 185(12):539
71. Hu Y, Yang J, Tian J, Jia L, Yu J-S (2014) Waste frying oil as a precursor for one-step synthesis of sulfur-doped carbon dots with pH-sensitive photoluminescence. Carbon 77:775–782
72. Li H, Sun C, Ali M, Zhou F, Zhang X, MacFarlane DR (2015) Sulfated carbon quantum dots as efficient visible-light switchable acid catalysts for room-temperature ring-opening reactions. Angew Chem Int Ed 54(29):8420–8424
73. Dong Y, Pang H, Yang HB, Guo C, Shao J, Chi Y, Li CM, Yu T (2013) Carbon-based dots co-doped with nitrogen and sulfur for high quantum yield and excitation-independent emission. Angew Chem Int Ed Eng 52(30):7800–7804
74. Guo L, Ge J, Liu W, Niu G, Jia Q, Wang H, Wang P (2016) Tunable multicolor carbon dots prepared from well-defined polythiophene derivatives and their emission mechanism. Nanoscale 8(2):729–734
75. Miao X, Yan X, Qu D, Li D, Tao FF, Sun Z (2017) Red emissive sulfur, nitrogen Codoped carbon dots and their application in ion detection and Theraonostics. ACS Appl Mater Interfaces 9(22): 18549–18556
76. Walekar LS, Zheng M, Zheng L, Long M (2019) Selenium and nitrogen co-doped carbon quantum dots as a fluorescent probe for perfluorooctanoic acid. Microchim Acta 186(5):278
77. Jia Y, Hu Y, Li Y, Zeng Q, Jiang X, Cheng Z (2019) Boron doped carbon dots as a multifunctional fluorescent probe for sorbate and vitamin B12. Microchim Acta 186(2):84
78. Barman MK, Jana B, Bhattacharyya S, Patra A (2014) Photophysical properties of doped carbon dots (N, P, and B) and their influence on Electron/hole transfer in carbon dots–nickel (II) Phthalocyanine conjugates. J Phys Chem C 118(34):20034–20041
79. Zuo G, Xie A, Li J, Su T, Pan X, Dong W (2017) Large emission red-shift of carbon dots by fluorine doping and their applications for red cell imaging and sensitive intracellular ag+ detection. J Phys Chem C 121(47):26558–26565
80. Yang S, Sun J, Li X, Zhou W, Wang Z, He P, Ding G, Xie X, Kang Z, Jiang M (2014) Large-scale fabrication of heavy doped carbon quantum dots with tunable-photoluminescence and sensitive fluorescence detection. J Mater Chem A 2(23):8660
81. Xu Q, Kuang T, Liu Y, Cai L, Peng X, Sreenivasan Sreeprasad T, Zhao P, Yu Z, Li N (2016) Heteroatom-doped carbon dots: synthesis, characterization, properties, photoluminescence mechanism and biological applications. J Mater Chem B 4(45):7204–7219
82. Wang M, Meng G (2016) Fluorescence "turn on" detection of Cr3+ using N-doped-CDs and graphitic nanosheet hybrids. RSC Adv 6(76):72728–72732
83. Peng J, Yin W, Shi J, Jin X, Ni G (2018) Magnesium and nitrogen co-doped carbon dots as fluorescent probes for quenchometric determination of paraoxon using pralidoxime as a linker. Microchim Acta 186(1):24
84. Lin L, Xiao Y, Wang Y, Zeng Y, Lin Z, Chen X (2019) Hydrothermal synthesis of nitrogen and copper co-doped carbon dots with intrinsic peroxidase-like activity for colorimetric discrimination of phenylenediamine isomers. Microchim Acta 186(5):288
85. Liu Y, Chao D, Zhou L, Li Y, Deng R, Zhang H (2018) Yellow emissive carbon dots with quantum yield up to 68.6% from manganese ions. Carbon 135:253–259
86. Wu W, Zhan L, Fan W, Song J, Li X, Li Z, Wang R, Zhang J, Zheng J, Wu M, Zeng H (2015) Cu-N dopants boost electron transfer and photooxidation reactions of carbon dots. Angew Chem Int Ed Eng 54(22):6540–6544
87. Cheng J, Wang C-F, Zhang Y, Yang S, Chen S (2016) Zinc ion-doped carbon dots with strong yellow photoluminescence. RSC Adv 6(43):37189–37194
88. Zhang HY, Wang Y, Xiao S, Wang H, Wang JH, Feng L (2017) Rapid detection of Cr(VI) ions based on cobalt(II)-doped carbon dots. Biosens Bioelectron 87:46–52
89. Li L, Wu G, Yang G, Peng J, Zhao J, Zhu J-J (2013) Focusing on luminescent graphene quantum dots: current status and future perspectives. Nanoscale 5(10):4015–4039
90. Tang L, Ji R, Li X, Bai G, Liu CP, Hao J, Lin J, Jiang H, Teng KS, Yang Z, Lau SP (2014) Deep ultraviolet to near-infrared emission and Photoresponse in layered N-doped graphene quantum dots. ACS Nano 8(6):6312–6320
91. Feng XT, Zhang F, Wang YL, Zhang Y, Yang YZ, Liu XG (2015) Luminescent carbon quantum dots with high quantum yield as a single white converter for white light emitting diodes. Appl Phys Lett 107(21):213102
92. Dang DK, Sundaram C, Ngo Y-LT, Chung JS, Kim EJ, Hur SH (2018) One pot solid-state synthesis of highly fluorescent N and S co-doped carbon dots and its use as fluorescent probe for Ag+ detection in aqueous solution. Sensors Actuators B Chem 255: 3284–3291

93. Qian Z, Ma J, Shan X, Feng H, Shao L, Chen J (2014) Highly luminescent N-doped carbon quantum dots as an effective multifunctional fluorescence sensing platform. Chem Eur J 20(8): 2254–2263
94. Lin L, Wang Y, Xiao Y, Liu W (2019) Hydrothermal synthesis of carbon dots codoped with nitrogen and phosphorus as a turn-on fluorescent probe for cadmium(II). Microchim Acta 186(3):147
95. Wang L, Zhu S-J, Wang H-Y, Qu S-N, Zhang Y-L, Zhang J-H, Chen Q-D, Xu H-L, Han W, Yang B, Sun H-B (2014) Common origin of green luminescence in carbon Nanodots and graphene quantum dots. ACS Nano 8(3):2541–2547
96. Yang Y, Hou J, Huo D, Wang X, Li J, Xu G, Bian M, He Q, Hou C, Yang M (2019) Green emitting carbon dots for sensitive fluorometric determination of cartap based on its aggregation effect on gold nanoparticles. Microchim Acta 186(4):259
97. Yang C, Thomsen RP, Ogaki R, Kjems J, Teo BM (2015) Ultrastable green fluorescence carbon dots with a high quantum yield for bioimaging and use as theranostic carriers. J Mater Chem B 3(22):4577–4584
98. Zhang J, Zhao X, Xian M, Dong C, Shuang S (2018) Folic acid-conjugated green luminescent carbon dots as a nanoprobe for identifying folate receptor-positive cancer cells. Talanta 183:39–47
99. Mohan R, Drbohlavova J, Hubalek J (2018) Dual band emission in carbon dots. Chem Phys Lett 692:196–201
100. Jiang K, Wu J, Wu Q, Wang X, Wang C, Li Y (2017) Stable fluorescence of green-emitting carbon Nanodots as a potential Nanothermometer in biological media. Part Part Syst Charact 34(2):1600197
101. Yang S, Sun X, Wang Z, Wang X, Guo G, Pu Q (2018) Anomalous enhancement of fluorescence of carbon dots through lanthanum doping and potential application in intracellular imaging of ferric ion. Nano Res 11(3):1369–1378
102. Pan X, Zhang Y, Sun X, Pan W, Yu G, Zhao Q, Wang J (2018) Carbon dots originated from methyl red with molecular state and surface state controlled emissions for sensing and imaging. J Lumin 204:303–311
103. Zhai Y, Wang Y, Li D, Zhou D, Jing P, Shen D, Qu S (2018) Red carbon dots-based phosphors for white light-emitting diodes with color rendering index of 92. J Colloid Interface Sci 528:281–288
104. Yan F, Bai Z, Zu F, Zhang Y, Sun X, Ma T, Chen L (2019) Yellow-emissive carbon dots with a large stokes shift are viable fluorescent probes for detection and cellular imaging of silver ions and glutathione. Microchim Acta 186(2):113
105. Li J, Zuo G, Pan X, Wei W, Qi X, Su T, Dong W (2018) Nitrogen-doped carbon dots as a fluorescent probe for the highly sensitive detection of Ag(+) and cell imaging. Luminescence 33(1):243–248
106. Jiang K, Sun S, Zhang L, Wang Y, Cai C, Lin H (2015) Bright-yellow-emissive N-doped carbon dots: preparation, cellular imaging, and bifunctional sensing. ACS Appl Mater Interfaces 7(41): 23231–23238
107. Ding YY, Gong XJ, Liu Y, Lu WJ, Gao YF, Xian M, Shuang SM, Dong C (2018) Facile preparation of bright orange fluorescent carbon dots and the constructed biosensing platform for the detection of pH in living cells. Talanta 189:8–15
108. Mutuyimana FP, Liu J, Nsanzamahoro S, Na M, Chen H, Chen X (2019) Yellow-emissive carbon dots as a fluorescent probe for chromium(VI). Microchim Acta 186(3):163
109. Xu Z, Wang C, Jiang K, Lin H, Huang Y, Zhang C (2015) Microwave-assisted rapid synthesis of amphibious yellow fluorescent carbon dots as a colorimetric Nanosensor for Cr(VI). Part Part Syst Charact 32(12):1058–1062
110. Wang W, Peng J, Li F, Su B, Chen X, Chen X (2018) Phosphorus and chlorine co-doped carbon dots with strong photoluminescence as a fluorescent probe for ferric ions. Microchim Acta 186(1):32
111. Qu S, Zhou D, Li D, Ji W, Jing P, Han D, Liu L, Zeng H, Shen D (2016) Toward efficient Orange emissive carbon Nanodots through conjugated sp(2) -domain controlling and surface charges engineering. Adv Mater 28(18):3516–3521
112. Song L, Cui Y, Zhang C, Hu Z, Liu X (2016) Microwave-assisted facile synthesis of yellow fluorescent carbon dots from o-phenylenediamine for cell imaging and sensitive detection of Fe3+ and H2O2. RSC Adv 6(21):17704–17712
113. Geng B, Yang D, Zheng F, Zhang C, Zhan J, Li Z, Pan D, Wang L (2017) Facile conversion of coal tar to orange fluorescent carbon quantum dots and their composite encapsulated by liposomes for bioimaging. New J Chem 41(23):14444–14451
114. Wang Y, Zhang Y, Jia M, Meng H, Li H, Guan Y, Feng L (2015) Functionalization of carbonaceous Nanodots from Mn(II) -coordinating functional knots. Chemistry 21(42):14843–14850
115. Dong Y, Chen Y, You X, Lin W, Lu C-H, Yang H-H, Chi Y (2017) High photoluminescent carbon based dots with tunable emission color from orange to green. Nanoscale 9(3):1028–1032
116. Sun Y, Wang X, Wang C, Tong D, Wu Q, Jiang K, Jiang Y, Wang C, Yang M (2018) Red emitting and highly stable carbon dots with dual response to pH values and ferric ions. Microchim Acta 185(1):83
117. Huang S, Yang E, Yao J, Liu Y, Xiao Q (2018) Red emission nitrogen, boron, sulfur co-doped carbon dots for "on-off-on" fluorescent mode detection of Ag(+) ions and l-cysteine in complex biological fluids and living cells. Anal Chim Acta 1035:192–202
118. Li C, Wang Y, Zhang X, Guo X, Kang X, Du L, Liu Y (2018) Red fluorescent carbon dots with phenylboronic acid tags for quick detection of Fe(III) in PC12 cells. J Colloid Interface Sci 526: 487–496
119. Sun S, Zhang L, Jiang K, Wu A, Lin H (2016) Toward high-efficient red emissive carbon dots: facile preparation, unique properties, and applications as multifunctional Theranostic agents. Chem Mater 28(23):8659–8668
120. Wang Z, Yuan F, Li X, Li Y, Zhong H, Fan L, Yang S (2017) 53% efficient red emissive carbon quantum dots for high color rendering and stable warm white-light-emitting diodes. Adv Mater 29(37)
121. Ding H, Ji Y, Wei J-S, Gao Q-Y, Zhou Z-Y, Xiong H-M (2017) Facile synthesis of red-emitting carbon dots from pulp-free lemon juice for bioimaging. J Mater Chem B 5(26):5272–5277
122. Jiang BP, Zhou B, Shen XC, Yu YX, Ji SC, Wen CC, Liang H (2015) Selective probing of gaseous Ammonia using red-emitting carbon dots based on an interfacial response mechanism. Chemistry 21(52):18993–18999
123. Ge J, Jia Q, Liu W, Guo L, Liu Q, Lan M, Zhang H, Meng X, Wang P (2015) Red-emissive carbon dots for fluorescent, photoacoustic, and thermal Theranostics in living mice. Adv Mater 27(28):4169–4177
124. Hou J, Wang W, Zhou T, Wang B, Li H, Ding L (2016) Synthesis and formation mechanistic investigation of nitrogen-doped carbon dots with high quantum yields and yellowish-green fluorescence. Nanoscale 8(21):11185–11193
125. Chen D, Wu W, Yuan Y, Zhou Y, Wan Z, Huang P (2016) Intense multi-state visible absorption and full-color luminescence of nitrogen-doped carbon quantum dots for blue-light-excitable solid-state-lighting. J Mater Chem C 4(38):9027–9035
126. Yang C, Zhu S, Li Z, Li Z, Chen C, Sun L, Tang W, Liu R, Sun Y, Yu M (2016) Nitrogen-doped carbon dots with excitation-independent long-wavelength emission produced by a room-temperature reaction. Chem Commun 52(80):11912–11914
127. Han L, Liu SG, Dong JX, Liang JY, Li LJ, Li NB, Luo HQ (2017) Facile synthesis of multicolor photoluminescent polymer carbon dots with surface-state energy gap-controlled emission. J Mater Chem C 5(41):10785–10793
128. Joseph J, Anappara AA (2017) White-light-emitting carbon dots prepared by the electrochemical exfoliation of graphite. ChemPhysChem 18(3):292–298

129. Liu ML, Yang L, Li RS, Chen BB, Liu H, Huang CZ (2017) Large-scale simultaneous synthesis of highly photoluminescent green amorphous carbon nanodots and yellow crystalline graphene quantum dots at room temperature. Green Chem 19(15):3611–3617
130. Hu S, Trinchi A, Atkin P, Cole I (2015) Tunable photoluminescence across the entire visible spectrum from carbon dots excited by white light. Angew Chem Int Ed Eng 54(10): 2970–2974
131. Li X, Zhang S, Kulinich SA, Liu Y, Zeng H (2014) Engineering surface states of carbon dots to achieve controllable luminescence for solid-luminescent composites and sensitive Be2+ detection. Sci Rep 4(1):4976
132. Dhenadhayalan N, Lin K-C, Suresh R, Ramamurthy P (2016) Unravelling the multiple emissive states in citric-acid-derived carbon dots. J Phys Chem C 120(2):1252–1261
133. Sun Z, Li X, Wu Y, Wei C, Zeng H (2018) Origin of green luminescence in carbon quantum dots: specific emission bands originate from oxidized carbon groups. New J Chem 42(6):4603–4611
134. Zheng Y, Yang D, Wu X, Yan H, Zhao Y, Feng B, Duan K, Weng J, Wang J (2015) A facile approach for the synthesis of highly luminescent carbon dots using vitamin-based small organic molecules with benzene ring structure as precursors. RSC Adv 5(110): 90245–90254
135. Yuan R, Liu J, Xiang W, Liang X (2018) Red-emitting carbon dots phosphors: a promising red color convertor toward warm white light emitting diodes. J Mater Sci Mater Electron 29(12):10453–10460
136. Fu M, Ehrat F, Wang Y, Milowska KZ, Reckmeier C, Rogach AL, Stolarczyk JK, Urban AS, Feldmann J (2015) Carbon dots: a unique fluorescent cocktail of polycyclic aromatic hydrocarbons. Nano Lett 15(9):6030–6035
137. Yuan B, Xie Z, Chen P, Zhou S (2018) Highly efficient carbon dots and their nanohybrids for trichromatic white LEDs. J Mater Chem C 6(22):5957–5963
138. Bao L, Liu C, Zhang Z-L, Pang D-W (2015) Photoluminescence-tunable carbon Nanodots: surface-state energy-gap tuning. Adv Mater 27(10):1663–1667
139. Hola K, Bourlinos AB, Kozak O, Berka K, Siskova KM, Havrdova M, Tucek J, Safarova K, Otyepka M, Giannelis EP, Zboril R (2014) Photoluminescence effects of graphitic core size and surface functional groups in carbon dots: COO− induced red-shift emission. Carbon 70:279–286
140. Ding H, Wei JS, Zhang P, Zhou ZY, Gao QY, Xiong HM (2018) Solvent-controlled synthesis of highly luminescent carbon dots with a wide color gamut and narrowed emission peak widths. Small 14(22):e1800612
141. Zhan J, Geng B, Wu K, Xu G, Wang L, Guo R, Lei B, Zheng F, Pan D, Wu M (2018) A solvent-engineered molecule fusion strategy for rational synthesis of carbon quantum dots with multicolor bandgap fluorescence. Carbon 130:153–163
142. Chen Y, Lian H, Wei Y, He X, Chen Y, Wang B, Zeng Q, Lin J (2018) Concentration-induced multi-colored emissions in carbon dots: origination from triple fluorescent centers. Nanoscale 10(14): 6734–6743